



UiT

THE ARCTIC
UNIVERSITY
OF NORWAY

Faculty of Biosciences, Fisheries and Economics
Department of Arctic and Marine Biology

Activity of XTHs during host plant infection by the parasitic plant *Cuscuta*

Adwoa Sarfowaa

BIO-3950 Master Thesis in Biology-May 2019



Activity of XTHs during host plant infection by the parasitic plant *Cuscuta*

Supervisors

Prof. Kirsten Krause

Dr. Stian Olsen

Department of Arctic and Marine Biology
Faculty of Biosciences, Fisheries and Economics

UiT The Arctic University of Norway

Table of Contents

List of Tables	vi
List of Figures.....	vii
Acknowledgements	viii
Abbreviations	ix
Abstract.....	1
1.0 Introduction	3
1.1 Parasitic Plants.....	3
1.1.1 Parasitic Plants and their behavior	4
1.2 The genus <i>Cuscuta</i> and its distribution.....	6
1.3 Susceptibility and resistance of hosts	8
1.4 Early Development Stages of <i>Cuscuta spp.</i>	9
1.4.1 Strategy and stages of host infection.....	10
1.5 The Plant Cell Wall.....	11
1.5.1 XTH modification in plants	11
1.5.2 XET Inhibitors	13
1.6 Aims and Objectives.....	14
2.0 Materials and Methods	16
2.1 Growth Site and Plant materials	16
2.2 Primer Design	16
2.3 Tissue harvesting and homogenization	18
2.3.1 RNA Isolation	18
2.3.2 Nucleic Acid Measurement.....	20
2.3.3 DNase Treatment	20
2.3.4 Gel Electrophoresis Analysis	22

2.3.5 Reverse Transcription (RT).....	24
2.3.6 Quantitative real-time PCR (qPCR).....	25
2.3.7 Assay Validation	28
2.3.8 Gene Expression Analysis.....	29
2.4 Quantification of XET Activity in <i>Cuscuta platyloba</i> and <i>Cuscuta campestris</i>	29
2.4.1 Xyloglucan Endotransglucosylase (XET) Dot Blot Analysis	32
2.5 Analysing the effect of Coomassie Brilliant Blue R250 on host <i>Cuscuta</i> infection.....	33
2.6 Cell Wall polysaccharides Analysis of <i>Cuscuta platyloba</i>	35
2.6.1 ELISA- Enzyme-linked immunosorbent assay of <i>Cuscuta platyloba</i>	35
3.0 Results	38
3.1 The expression of <i>Cr-XTH</i> homologues in <i>Cuscuta campestris</i> and <i>Cuscuta platyloba</i>	38
3.2 RT-qPCR analysis of <i>Cr-XTH</i> homologue in <i>C. campestris</i> and <i>C. platyloba</i>	39
3.3 Primer Efficiencies	41
3.4 Gene Expression of <i>XTH-1</i> and <i>XTH-2</i> in <i>Cuscuta campestris</i> and <i>Cuscuta platyloba</i>	43
3.5 The Activity levels of xyloglucan endotransglucosylases from <i>C. campestris</i> and <i>C. platyloba</i>	45
3.5.1 The Bovine Serum Albumin (BSA) standards and regression equation	45
3.5.2 XET activity in <i>C. platyloba</i> and <i>C. campestris</i> during <i>P. zonale</i> infection.....	46
3.6 The parasitization of <i>Pelargonium zonale</i> coated with BB-R250 and control.....	49
3.7 Enzyme Linked Immuno-Sorbent Assay (ELISA) analysis on <i>Cuscuta platyloba</i>	52
4.0 Discussion.....	53
4.1 Extraction influence on results	53
4.2 The Gene Expression of XTHs and XET activities in the <i>Cuscuta</i> tissue samples.....	54
4.3 Infection Trials with Coomassie Brilliant Blue R 250 (BB-R250)	57
4.4 Abundance of Xyloglucan in the <i>Cuscuta</i> cell wall	57

5.0 Conclusion 59

 5.1 Outlook 59

6.0 References 60

7.0 Appendix I 66

7.1 Appendix II 67

7.2 Appendix III 68

7.3 Appendix IV 69

7.4 Appendix V 71

List of Tables

Table 1- Population estimates of higher plant species, parasitic plant species and other plant species with other heterotrophic lifestyles.	4
Table 3- Reaction component for DNase Treatment.....	21
Table 4- Total reaction volumes (μL) of <i>Cuscuta</i> tissue samples used for Gel Electrophoresis Analysis.	23
Table 5- First reaction step for Reverse Transcription.	24
Table 6- Second reaction step for Reverse Transcription.	25
Table 7- 100-fold cDNA Dilution from original samples.	26
Table 8- Real-time PCR Reaction mastermixes of volume, 20 μL /tube for each <i>Cuscuta</i> tissue sample.....	27
Table 9- Program set-up for Primer Optimisation.....	27
Table 10- Reaction setup for Assay Validation Analysis.....	28
Table 11- Reaction setup for the Gene Expression Analysis.	29
Table 12- The Dilution scheme for BSA Standard Assays of volume 100 μL	30
Table 13- Total Weight of <i>Cuscuta</i> tissue sample and the volume of ice-cold extraction buffer required.....	31
Table 14- The efficiencies of PCR calculated from the respective standard curves.	43
Table 15- The quantitative estimation of the amount of protein extracts present in the unknown solution of <i>C. platyloba</i> and <i>C. campestris</i> tissue samples.	46
Table 16- Mean separation was completed using Tukeys procedure ($\alpha=0.05$).....	48
Table 17- Frequency of impeded <i>C. platyloba</i> infections on coated <i>P. zonale</i> petioles.	51

List of Figures

Figure 1- (a) - the photo of parasitic plant.....	5
Figure 2- The <i>Cuscuta</i> genus infecting its susceptible host <i>P. zonale</i>	7
Figure 3- Global distribution map of <i>Cuscuta</i> species.	8
Figure 4- Labelled regions of the XET Test papers which guided blotting pattern	33
Figure 5- Experimental set up of coated <i>Cuscuta</i> petioles tissues.	35
Figure 7- Melt peaks of RT-qPCR amplicons.	40
Figure 8- The standard curves for all tested genes.	42
Figure 9- The expression level of gene XTH1 and XTH2 from <i>C. campestris</i> and <i>C. platyloba</i> against the normalisation of all the four reference genes.	44
Figure 10- Graphical Representation of Bovine Serum Albumin (BSA) standards.....	45
Figure 11- Comparison of the level of XET activity of the haustorium and stem in <i>C. platyloba</i> and <i>C. campestris</i>	47
Figure 12- Bar Graph representation of XET Activity in <i>C. platyloba</i> and <i>C. campestris</i>	48
Figure 13- Microscopical cross-sectional views <i>C. platyloba</i> on the <i>P. zonale</i> , host petioles coated with BB-R250.....	50
Figure 14- Microscopical cross-sectional views <i>C. platyloba</i> on the <i>P. zonale</i> , host petioles coated with 0.005% Poly-L-Lysine.	51
Figure 15- The molecule detected by MAb was Xyloglucan.....	52

Acknowledgements

“If it had not been the Lord who was on my side, where will I have been” My greatest gratitude goes to God Almighty for His numerous mercies, protection and a successful end in my master’s studies. My sincere appreciation again goes to Her Hon. Lady Sarah Adwoa Sarfo, Mad. Sonia Nkum, and Mrs. Phillipa Lamptey for their help to pursue further into my academic journey. I wish to express my sincere gratitude to my supervisors, Prof. Kirsten Krause and Dr. Stian Olsen for all of their guidance, support, patience to assist me at all times and introducing me this project. Their contributions toward the success of my studies are invaluable. I would also like to thank all the Microorganisms and Plants Research Group, most especially Alena Didriksen and Andrew Galloway for their insight, extra guidance and providing lab. materials. Stian your suggestions always brought me hope and confidence to overcome any problems.

As this thesis was undertaken in the lab. of the Department of Arctic and Marine Biology, this project would have not have been possible without such laboratory facilities. I am thankful to Siv Andreassen (Senior Advisor) and all my external sensors for their support towards completion of this project. A special thanks to my family, friends (Joel Abbey and Kenneth Eteme Anku) and all who contributed to this success for their support and unconditional love and encouragement.

Abbreviations

µg	microgram
µL	microlitre
0.1 M DTT	Dithiothreitol
3,3,5,5-TMB	3,3,5,5 Tetramethylbenzidine
AIR preparation	Alcohol Insoluble Residue
au	Level of fluorescence
BB-R250	Coomassie Brilliant Blue R250
BSA	Bovine Serum Albumin
Buffer RL T	Guanidine Isothiocyanate
CaCl	Calcium Chloride
CcH	<i>Cuscuta campestris</i> haustorium
CcS	<i>Cuscuta campestris</i> stem
cDNA	Complementary Deoxyribonucleic acid
CpH	<i>Cuscuta platyloba</i> haustorium
CpS	<i>Cuscuta platyloba</i> stem
dNTP	Deoxyribonucleotide triphosphate
EDTA	Ethylenediaminetetraacetic acid
ELISA	Enzyme-Linked Immuno-sorbent Assay
EtOH	Ethanol
F primer	Forward primer
g	gram
H	Haustoria tissue sample
HRP	Anti-rat horse radish peroxidase
Kb	Kilobase
KOH	Potassium hydroxide
mAb	Monoclonal Antibody

mg	milligram
MM	Mastermixes
ms	millisecond
NaCl	Sodium Chloride
ng	nanogram
nm	nanometre
Oligo (dT)₁₈	Single-stranded sequence of deoxythymine
PBS	Potassium Salt
qPCR	Quantitative real-time Polymerase chain reaction
R primer	Reverse primer
RNA	Ribonucleic Acid
rpm	Revolutions per minute
S	Stem tissue sample
TAE Buffer	Tris-acetate-EDTA Buffer
V	Volt
Vol.	Volume
XEH	Xyloglucan endohydrolases activity
XET	Xyloglucan endotransglucosylase activity
XTHs	Xyloglucan endotransglucosylases/hydrolases
XyGO-SR	Sulforhodamine-labelled xyloglucan oligosaccharide
β – ME	β – Mercaptoethanol

Abstract

Parasitic plants including *Cuscuta* develop specialized structures called haustoria during infection. These specialized organs give the parasite the capacity of host attachment, invasion, vasculature connection and material transfer between the host and the parasite. Successful invasion allows organic substances, nutrients and water to flow into the parasite through the host phloem and xylem cells. Invading the host plant requires a number of cell wall modifications and recent findings suggests that, a number of enzymes and cell wall components control the modification process in the formation of haustoria. The cell wall-modifying enzymes xyloglucan endotransglucosylases/hydrolases (XTHs) have been related to *Cuscuta reflexa* haustoria formation. In the presented thesis, the infection mechanism of other *Cuscuta* species was examined by investigating the expression and activity of XTHs during host infection. Also, the effect of an XTH enzyme inhibitor on host plant infection was tested. *Cuscuta campestris* and *Cuscuta platyloba* were grown on the host plant *Pelargonium zonale* to quantify the expression of XTHs as well as the XET activities in the haustoria and stems of the parasite. RNA extraction and qPCR analysis were used for quantifying the gene expression of *Cr-XTH* homologues. An ELISA assay was used to analyze the cell wall component in the *Cuscuta* species. Furthermore, an inhibition trial on *Cuscuta* species and the host plant was conducted using Coomassie blue BB-R250 at 5mM concentration. Results showed that the expression of *Cp-XTH1* was well regulated in the haustoria of *C. platyloba*, but not in *C. campestris*, while the expression of *Cc-XTH2* was greatly regulated in *C. campestris* but not in *C. platyloba*. XET activity was generally higher in *C. campestris* than *C. platyloba* but possessed higher levels of XET in their haustoria and stems than that of *C. platyloba* per mg tissue sample. Furthermore, the ELISA assay showed that xyloglucan content was high in both the haustoria and the stem. The higher xyloglucan levels in the haustoria section of *C. platyloba* coordinated with the high expression of XTHs and activity of XET per mg of the tissue samples but vice versa with the activity levels of XET per mg of the protein concentration. The high expression of XTHs and XET was correlated to high xyloglucan levels in the haustoria. The infection trial of *C. platyloba* infecting *P. zonale* coated with Coomassie blue BB-R250 revealed that the preventive infection by 5 Mm concentration was 6 times higher than in the absence of dye (0 mM). In conclusion, the expression of XET in *Cuscuta* species is not dependent on the different groups of XTH. Therefore, once XTH is expressed, then the activity and levels of XET increases irrespective of the groups within the various species. Some preventive penetration was

recorded although it was not of high percentage (15.8%) during the inhibition infection trial of Coomassie blue BB-R250. Therefore, the high levels of XTH, XET and xyloglucan work synergistically to modify the parasitic plant leading to the formation of the specialized structures called haustoria.

Keywords: Parasitic plants, *Cuscuta* species, Haustorium, XTHs, XET Activity.

1.0 Introduction

1.1 Parasitic Plants

In ecology and biology, the existence of biotic and abiotic factors constantly influences all life forms including plants which contribute to the stability of the ecosystem. The concept of plant existence and diversification points out that plants dominate different ecological niches and these plant-niche composition ranged from the monotypic gymnosperm genus *Welwitschia* in the desert to the smallest flowering plants, *Wolffia* species in the aquatic environment. It further comprises the carnivorous plant, Venus flytrap and the most popular scientific model plant, *Arabidopsis*. Poulin (2011) defined parasitic plants as plants that, through a direct physical connection, acquire resources from another plant (the host) at the expense of the latter. The main purpose of parasitization of a host plant is to derive water and nutrients through the connection of the haustoria to the xylem and phloem (Begon et al. 2006). However, this mechanism can exert a positive influence on the host plant (Runyon et al. 2008): some plant hormones such as salicylic acid protects tomato plant against insect herbivores.

Superficially, there have been very close morphological resemblance in some parasitic plants. Bidartondo (2005) cleared the scientific conflict of myco-heterotrophic plants to be root parasite during its early life cycle. The mutualistic evolvement of the epiphyte plants (plants that live on the surface of the other without feeding on them) and myco-heterotrophic plants (other plants that survive on the interaction with soil-borne fungi, example: *Fusarium oxysporum*) are not classified as parasitic plants (Merckx et al. 2009). Hence, considering their mode of transfer of nutrients and water from the host to the myco-heterotrophic plants without the haustoria as media of transfer reject them as parasitic plants.

Parasitic plants generally originated within the angiosperms and have developed independently from 12 to 13 events (Westwood et al. 2010). The global parasitic plants population is about 4000 species, which corresponds to around 1% of the dicotyledonous angiosperm species (Westwood et al. 2010; Barkman et al. 2007).

Table 1- Population estimates of higher plant species, parasitic plant species and other plant species with other heterotrophic lifestyles.

Category	Number of species
Angiosperms	Estimated 250 000 species (Wikström et al. 2001)
Myco-heterotrophic plants (achlorophyllous)	Over 400 species (87 genera) (Leake 1994)
Partially myco-heterotrophs	20 000 species (Merckx et al. 2009)
Parasite angiosperms	Around 4500 species among 20 families (390 holoparasitic species: 4100 hemiparasitic species) (Heide-Jørgensen 2008)
Carnivorous plants	Over 600 species (Ellison and Gotelli 2009)
Genus <i>Cuscuta</i>	150-200 species (McNeal et al. 2007)

NOTE: The table was adopted from Furuhashi et al. (2011).

Studies about the lifestyle of parasitic plants and several evolutionary events has led to a diversity in morphology that has greatly assisted to develop the phylogenetic tree with links to the Orders in the parasitic genera.

1.1.1 Parasitic Plants and their behavior

The host plant parts that are infected by a parasite provides the guideline to the categorization of parasitic plants. The most fundamental distinction is based on whether they grow above or below ground. Parasites that infect the above ground parts of a host are referred to as shoot parasites, the others are root parasites. A distinctive characteristic of all parasitic plant is the presence of a nutrient sucking channel called haustorium.

Haustor or *haurire*, the Latinised name for haustorium means “water drawer” and it is described by Yoshida et al. (2016) as “a specialized organ for host attachment, invasion, vasculature connection and material transfer between the host and the parasite.” The nutrient-absorbing structure of biotrophic plant-pathogenic fungi such as the rust fungi (Basidiomycota) and powdery

mildew fungi (Ascomycota) have invasive organ similar to the haustoria in parasitic plants. Both differ, however, morphologically and structurally in two main aspects.

The haustorium of a parasitic plant is a multicellular organ but fungal haustorium is a unicellular organ. While the latter grows intracellularly and is protected by a host-derived extrahaustorial membrane, the parasitic plant haustorium is an intercellular organ that gradually infuses in the host and therefore make a host-parasite connection (Mayer 2006). The acquisition of nutrients from the host is successful by the haustoria-vascular bundles connections (Kaiser et al. 2015). Within this are continuous phloem or xylem cells that allow the functional flow of macro-molecules between the host and parasite. The transfer of amino acids, organic acids, inorganic ions and water to the parasite is through the host xylem whilst the usable organ for the flow of sugar, ions and amino acids is the host phloem (Hibberd and Dieter Jeschke 2001).

The formation of some specialized structures such as the interspecific plasmodesmata further aid in cell-to-cell connectivity aside the haustoria in *Cuscuta* (Birschwilks et al. 2006). Hence, there are still unestablished findings on the exact mode and selectivity of the solute exchange.

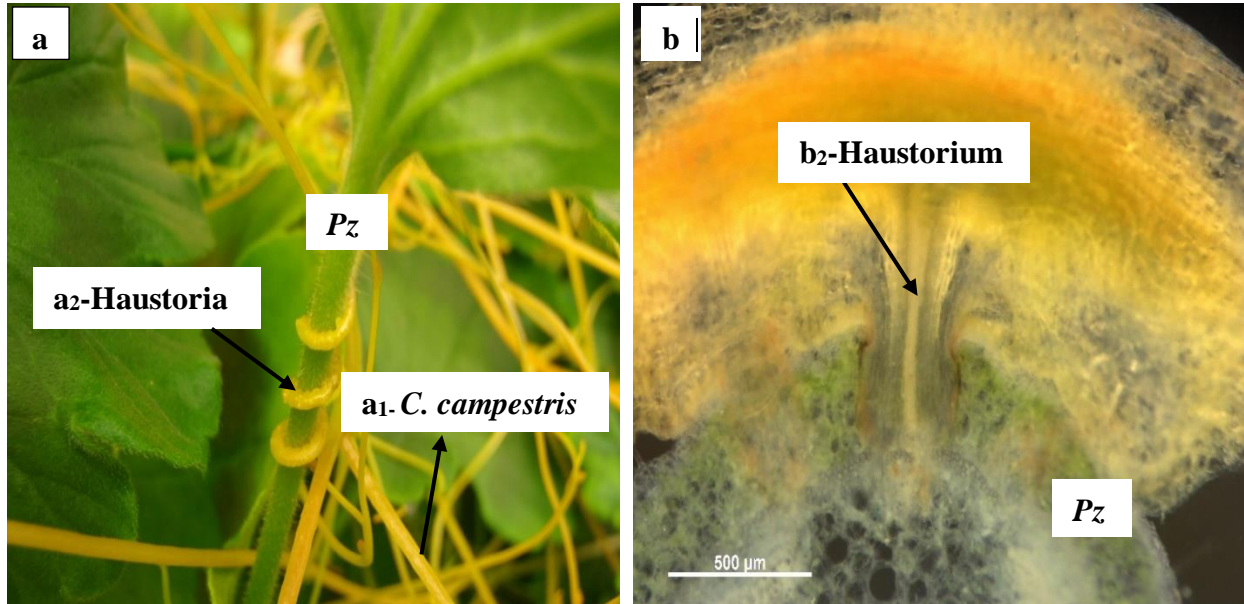


Figure 1- (a) - the photo of parasitic plant, (a₁) *Cuscuta campestris* and its (a₂) haustorium penetrating a host (arrow). (b/b₂)-The microscopical cross-section of a haustorium successfully fused into its compatible host, Pz - *Pelargonium zonale*. Scale bar = 500 μM.

Parasitic plants are also grouped into obligate and facultative parasites in relation to their dependency on the host to complete their life cycles. Obligates fully rely on host plants during their entire life cycle while those known as facultative could live without host plants (Yoshida and Shirasu 2012). Their levels of photosynthetic activities can also be used to classify parasitic plants, and these are hemiparasites and holoparasites. Parasitic plants that could generally photosynthesize their own food but rely partly on host plant is known as hemiparasites. They only rely on their host to derive non-photosynthetic solutes such as inorganic nutrients and water. On the other hand, holoparasites behaviour is directly opposite to that of other species as they are incapable of photosynthesizing their own food.

Relating the different lifestyles of parasitic plants, hemiparasites can be further categorized into being facultative or obligates. Examples are facultative root hemiparasite (Yellow rattle) and obligate stem hemiparasite (Mistletoe). Holoparasites, in contrast, is linked to only obligate lifestyle and examples are stem holoparasite (Dodder) and root holoparasites (*Hydnora* species).

1.2 The genus *Cuscuta* and its distribution

The focus of this study is a group of parasitic plants known as *Cuscuta* and it is therefore important for detailed introduction of the genus. *Cuscuta* belongs to the family Convolvulaceae, commonly referred to as the morning glory family. It is a vine-type parasite (Press and Phoenix 2005) and consists of about 200 species which are described as obligate stem holoparasites (García et al. 2014) and it is a close descendant (McNeal et al. 2007).

In the *Cuscuta* genus, the morphological characteristics of the stigma and style further subdivide it into three subgenera which include *Monogyna*, *Cuscuta* and *Grammica* (McNeal et al. 2007). Dawson et al. (1994) clearly described the stem of *Cuscuta reflexa*, a member of the clade *Monogyna* as thick but *Cuscuta campestris* of the subgenus *Grammica* as thin and delicate. In the subgenus, *Grammica* is mainly divided into two; *Eugrammica* and *Cleistrogrammica* (Stefanović et al. 2007).

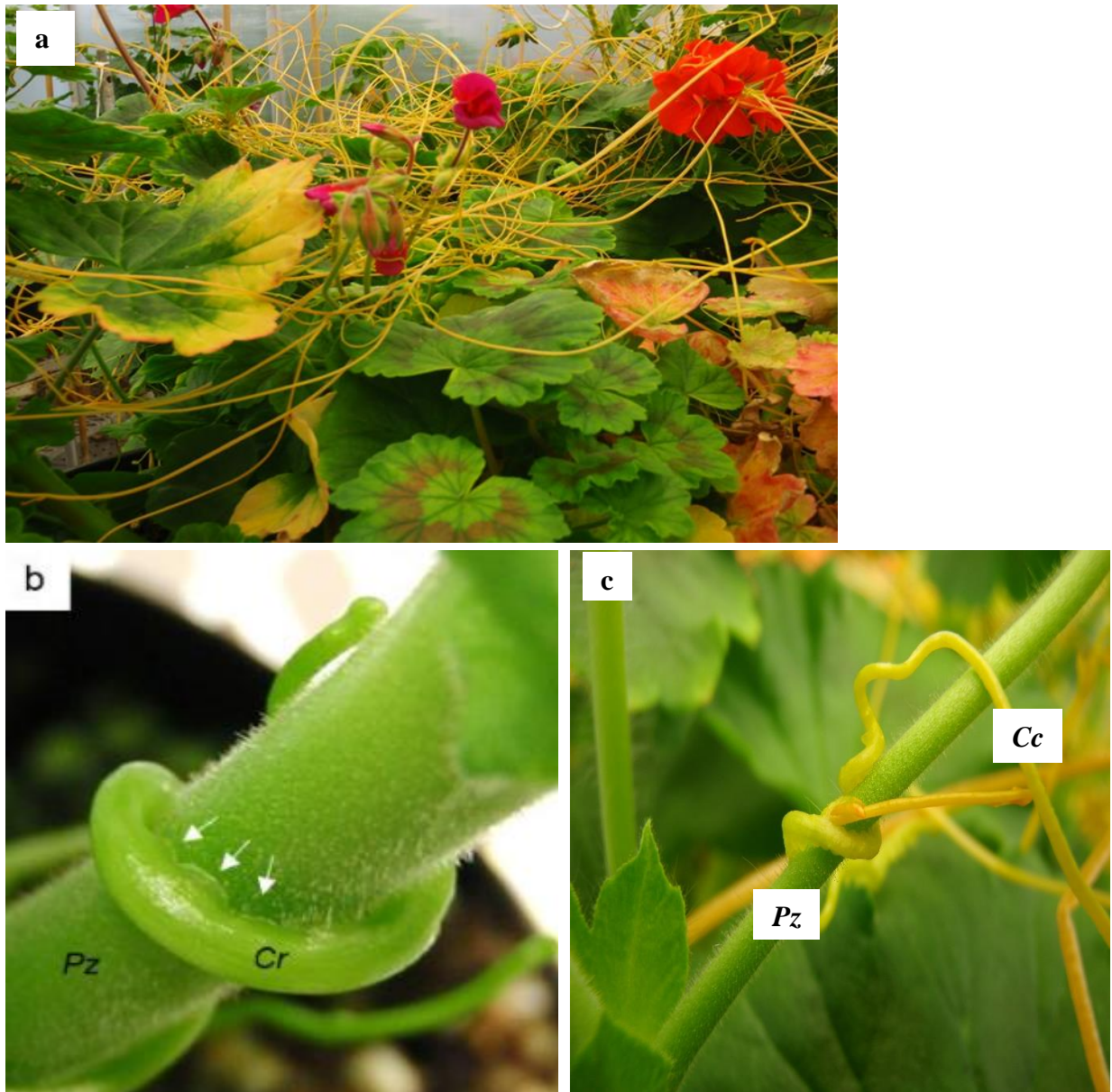


Figure 2- The *Cuscuta* genus infecting its susceptible host *P. zonale*. (a) - stem of *Cuscuta campestris* (*Cc*) (b) Infusion of *C. reflexa* (*Cr*) on *P. zonale* (*Pz*) (arrow), (c) Infusion of *C. campestris* (*Cc*) on host, image taken by Stian Olsen.

The *Cuscuta* species are reported to be globally spread and their distribution include every continent except the Antarctica. They are highly populated in the tropical and subtropical areas whereby approximately 150 species (75%) are abundant in the Americas (Yuncker 1932; Stefanović et al. 2007).

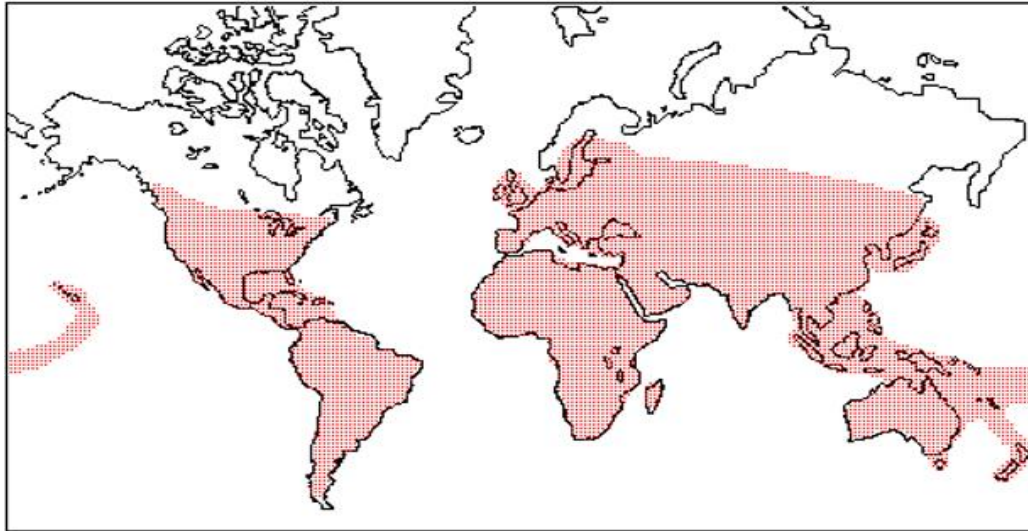


Figure 3- Global distribution map of Cuscuta species. (www.parasiticplants.siu.edu/Cuscutaceae/)

1.3 Susceptibility and resistance of hosts

The signs of active plant responses to parasitic infection can be grouped into three main forms which are susceptibility action, resistance action and dual-response actions. Host-parasite susceptibility action is reported in Hegenauer et al. (2016) which confirmed the infection of *C. reflexa* as highly compatible with wild tomato, *Solanum pennelli* and *Pelargonium zonale*. For this reason, both plants are mostly used in host-parasite interaction experiments.

Regardless of the arrangement of vascular bundles of monocotyledonous plants which strongly restrict interspecies connections with *Cuscuta* species. *Cuscuta australis* on the other hand successfully breaks this incompatibility boundary or the inhibitory actions of the cell wall of the host making it susceptible (Dawson et al. 1994).

Many host plants specifically use wound-seals to block the penetration of *Cuscuta* haustoria infection actions to host's vascular bundles and automatically cause disintegration. This is typical for the interactions between *Cuscuta* species and host such as the *Malvaceae* species *Gossypium hirsutum* and *Hibiscus rosa-sinensis* (Capderon et al. 1985). Kaiser et al. (2015), also recorded a host cell modification action in *Solanum lycopersicum* at infection site which is controlled by the elongation and bursting of the host epidermal cells the early stages of haustoria development of *C. reflexa*. The cell elongation process is influenced by the expression of genes such as aquaporins

(Werner et al. 2001) and some cell wall modification enzymes like Xyloglucan endotransglucosylases/hydrolases (Albert et al. 2004).

The resistance of *S. lycopersicum* to *C. reflexa* is not extended to species like *Cuscuta pentagona*, *Cuscuta suaveolens* and *Cuscuta europaea* (Ranjan et al. 2014; Jiang et al. 2013). Nevertheless, the induction of the haustoria of *C. pentagona* into *S. lycopersicum* releases two stress hormones called Salicylic acid (SA) and Jasmonic acid (JA) (Runyon et al. 2010).

Dual-response actions can be recorded during the attack of *C. reflexa* to the tropical liana *Ancistrocladus heyneanus*. Parasitism is successful at an early stage but the host defence activities renounce its successfulness and subsequently causes haustoria degeneration (Bringmann et al. 1999). Again, studies by Christensen et al. (2003) showed a partial resistance action of *C. reflexa* and *C. japonica* by enhancing the localized bark outgrowths that force out the infection organs but the parasites subsequently produce new infection sites.

1.4 Early Development Stages of *Cuscuta* spp.

Cuscuta is an annual species that grows mainly by seed but to a lesser extent it can also reproduce by shoot fragments (Albert et al. 2008). The seeds possess hard seed coats that enable them to thrive in soils for many years. The dormancy of these seeds are broken as a result of soil microbial activities, weathering or grazing, thus allowing these seeds to germinate and survive in or near the surface of soils (Mishra et al. 2006). These seedlings are rootless and leafless on their stems. During this early stage, the seedlings are often green in colour showing the presence of chlorophyll. However, the amount of chlorophyll present in these seedlings are less and therefore it cannot survive on its own for long. After germination, the *Cuscuta* seedling lives normally for less than 3 weeks before becoming parasitic (Furuhashi et al. 2011).

The *Cuscuta* seedling on its own cannot absorb water and CO₂ because of the low levels of Rubisco and chlorophyll. Initially the green colour possessed by the seedling changes into orange or purple after parasitization. These colour changes observed in *Cuscuta* spp. after parasitization is an underlining fact, that the plant gains energy from a host plant and does not need to photosynthesize (Furuhashi et al. 2011). Therefore, the need for survival of *Cuscuta* spp initiates the search for a host plant.

1.4.1 Strategy and stages of host infection

Host plants attract *Cuscuta* by releasing volatiles which are recognized as chemo-attractants. This serves as guide for seeding growth and increases the incidence of infections (Runyon et al. 2006). A detailed analysis from Kaiser et al. (2015), identifies that tomato produces terpenoids (α -pinene, β -myrcene, and β -phellandrene) as volatile compounds and this serves as chemical cues or chemo-attractants for *Cuscuta spp.*

The first physical contact after identifying an appropriate host is the attachment phase, which is facilitated by haustoria hairs or the prehaustoria (Yoshida et al. 2016; Albert et al. 2008). The haustoria hair enables the parasite to anchor its stem unto the surface of the host plant. The elliptic haustoria shape with a wedge-like tip begins to form from the inner side of the stem coiled around its host. Prehaustoria formation causes an accumulation of starch and nuclei enlargement within the cortex and this leads to cell division of the epidermal cells. The elongation of the epidermal cells leads to the formation of “haustoria hairs” which secretes hemi-cellulose, pectinaceous mucilage-like material that establishes structural bond with the host surface (Yoshida et al. 2016). Albert et al. (2008) states that, *Cuscuta* does not only secrete pectin or sticky substances, but it also induces the host plant to secrete attachment-enhancing substances such as arabinogalactan proteins (Kaiser et al. 2015). The host cells close to the point of contact respond by a high spike in cytosolic calcium accumulation which can last for about 48 hours. Cytosolic calcium accumulation forms part of the signal transduction pathway of plant response to a number of stimuli such as touch or defense triggers. However, there has been no clear reason for this high calcium spikes (Kaiser et al. 2015).

After the attachment phase, the next phase is the penetration phase as the prehaustoria makes its way into the host stem Yoshida et al. (2016) . *Cuscuta*, on its way to have a drink overcomes the host tissue through the fissure in the host stem. This process is supported by the activities of hydrolytic enzymes such as methylesterases, pectinase or loosening particles (Yoshida et al. 2016; Albert et al. 2008) which enable the haustoria to penetrate the host stem.

After a day or two, cells at the tip of the haustoria begin to elongate into “searching hyphae”. These searching hyphae are tip-growing cells that possess large nucleus and Golgi derived vesicles necessary for elongation. The searching hyphae grow until they locate the xylem or phloem cells of the host. Once it establishes contact with these cells, interspecies plasmodesmata connections

are formed along the walls of the tip of the searching hyphae (Yoshida et al. 2016). Upon contact with the sieve cells, the searching hyphae grow around the cell like the fingers of a hand (Kaiser et al. 2015). This causes the parasitic cell in contact with the host cell to grow about 20 times its size (Kaiser et al. 2015; Albert et al. 2008). This differentiates the cells into an ambivalent character, as they function as both a sieve cell and a transfer cell. The plasmodesmata connections create a cytoplasmic syncytium by which the host plant supplies the parasite with water, nutrient, carbohydrates, among others (Yoshida et al. 2016; Albert et al. 2008).

1.5 The Plant Cell Wall

The plant cell wall is a unique component of the plant structures that plays significant roles to the survival of the plant. The ultimate function of the plant cell wall is protection and interaction with the environment (Chebli and Geitmann 2017). Plants are made up of 35 different types of cells which are distinct from each other in terms of their position, shape, size and characteristics. The cell wall layers are typically thin (0.1 - 1µm) and consist of complex polysaccharides and sufficient amount of structural proteins (Cosgrove 2005).

1.5.1 XTH modification in plants

Over the years, the primary cell wall is believed to have evolved and contains cellulose microfibrils entwined in a matrix of structurally varied hemicellulose and pectin polysaccharides with some additional protein structures (Rose et al. 2002). The hemicellulose component of the cell wall include xyloglucans, xylans, mannans and glucomannans, and β -(1→3,1→4)-glucans which is absent in all terrestrial plants (Scheller and Ulvskov 2010; Mota et al. 2018). Xyloglucan (XyG) is the most abundant hemicellulose in the primary walls of dicots and conifers. Xylan is identified to dominate 20% of the primary cell wall and mannans and glucomannans (noted to play the role of seed storage compounds) constitution in all cell walls is unspecific but reported to higher in land plants, mosses and lycophytes (Scheller and Ulvskov 2010).

Cell defense against pathogens is a critical aspect in cell wall construction. Therefore, it is believed that the main components responsible for the major tension-bearing structure of the primary cell wall is the cellulose and hemicellulose xyloglucans (Rose et al. 2002; Muñoz-Bertomeu and

Lorences 2014). A possible pathogen entry or invasion implies a breakdown in the defense structure of the primary cell wall of the plants. Evidence from other researches points to the enzymatic activities of invading pathogens which causes the breakdown on the primary cell walls of plant (Muñoz-Bertomeu and Lorences 2014).

The synthesis of the plant cell wall follows a unique structure and mechanism. Xyloglucans bonds non-covalently to cellulose and this act as the major tensile strength of the primary cell structure. These together comprise about two thirds of the dry mass of the cell wall. Therefore, enzymes mobilizing xyloglucans may act as major agents controlling wall strength and expansion (Rose et al. 2002). These processes involve the activities of enzymes which integrates newly formed matrix polysaccharides into an already existing network thus aiding in the process of expansion and cell wall assemblage (Sharples et al. 2017; Cosgrove 2005). These enzymes are broadly known as Endotransglycosylases, which cut and join ligate glycans together. This large family comprises of a number of XTH groups; example, 33 XTHs in *A. thaliana* (Chormova et al. 2015) which may perform the same function or slightly different functions. These functional genes have been broadly grouped into three, depicting the phylogenetic relationship between their members (Yokoyama and Nishitani 2001). Example of such subfamilies are *At-XTH1* and *At-XTH2* and it has been described by Okazawa et al. (1993) that, the latter are closely related and belong to the “Group 1” gene family in XTHs. Biochemically, each member in “Group1” has shown to mediate only transglucosylation between xyloglucans in vitro (Xu et al. 1996; Nishitani and Tominaga 1992). Moreover, Campbell and Braam (1999) reported that, enzymatic action is not specific within each XTH subfamily and hence several different genes encode similar enzymic activities.

Xyloglucan endotransglucosylase (XET) is one such activity that cuts and rejoins xyloglucans to form glycosidic bonds with other xyloglucan end chains (Cosgrove 2005). Xyloglucan endohydrolases (XEH) is basically another activity that occurs in the large family of enzymes called xyloglucan endotransglucosylase/hydrolase (XTHs) (Rose et al. 2002; Muñoz-Bertomeu and Lorences 2014).

However, mRNA quantification analysis was conducted by using real-time PCR where the study revealed that, most functions of XTH gene family are specific to organ-or-tissue expression profiles such as members in “Group2” are predominantly expressed in roots while individual XTH genes are regulated in diverse ways to plant hormones. One such group is the *SkXTH1* proteins, which

functions like XET over a broad range of temperature and pH range (Van Sandt et al. 2007). Other members of the family such as the xyloglucan hydrolase (XEH) use water as substrate, which results in xyloglucan hydrolysis (Van Sandt et al. 2007).

According to Cosgrove (2005), the wall strengthening ability by XET has been experimentally proven and that XET grafts xyloglucans onto other structures or chains that are already part of the wall. This contributes to the strengthening mechanism and the extensibility of the plants.

At the site of invasion, pathogenic enzymes degrade the various components of the cell wall causing loosening among the different constituents of the cell wall components. Muñoz-Bertomeu and Lorences (2014), reports that, depolymerization of the hemicellulose and xyloglucan are the major causes that results in the breakdown of the plant cell wall. This occurs because the activities of XET reduce drastically during the infection process and this further deteriorates affecting the XTHs as the infection progresses (Muñoz-Bertomeu and Lorences 2014). This mechanism may differ from one plant to the other due to the composition of polymers within the plant. Therefore, the different polymers playing different roles which may differ in the infection process (Muñoz-Bertomeu and Lorences 2014). Consequently, preventing spiked levels of XTH in parasitic stems as a control measure will prevent haustoria formation thus avoid invasion by the parasite plant (Olsen and Krause 2017).

1.5.2 XET Inhibitors

As a counter measure to prevent the invasion by plant pathogens, research has scratched the surface into the generation of XET inhibitors. Xenobiotics, as they are popularly called, have been identified to limit the activities of XET in plant tissues. Chormova et al. (2015), reports that, among the eight xenobiotics selected only two namely; vulpinic acid and brilliant blue G were the best performing xenobiotics that had effect on XET. However, results from points to the fact that, these xenobiotics does not completely inhibit the activities of XET in parasitic plants (Olsen and Krause 2017). Nevertheless, the quantity, natural phenomenon and chemical concentration were some key contributors to the successes and failures observed in these experiments (Olsen and Krause 2017; Chormova et al. 2015).

1.6 Aims and Objectives

As a build-up to further investigate some aspects of these findings, the experiments executed in this thesis aim at understanding the infection mechanisms of *Cuscuta* by investigating the activity of XTHs during host infection and the effects of enzymes inhibitors. There has been broad compilation about the study of XTHs among a large numbers of plant species, but limited information is available in terms of the *Cuscuta* genus. Moreover, the knowledge from this study will broaden the scope of *Cuscuta* cell wall reports available and further help to establish the dynamics of expression in cell wall components and their modifiers specifically in *Cuscuta campestris* and *Cuscuta platyloba*. Therefore, the hypotheses (1 to 3) and objectives (a, b) of this research are to;

1. The expressions and activity levels of XTHs and XET in both *C. campestris* and *C. platyloba* have different but measurable effects on haustoria formation. On this account, the objectives are to;
 - a. Analyze expression of *Cr-XTH* homologues in *Cuscuta campestris* and *Cuscuta platyloba*.
 - b. Quantify XET activity during haustorium development in *C. campestris* and *C. platyloba*.

2. Coomassie Brilliant Blue R 250 has a measurable effect on *C. platyloba*, thus the objectives are to;
 - a. Co-culture coated *P. zonale* petioles with *C. platyloba* shoots.
 - b. Quantify the infection attempts according to successful (host penetration) and unsuccessful attempts.

3. The xyloglucan component of hemicellulose is contained in equal proportions in the cell wall of *C. platyloba* and its analysis will be involved in the use the monoclonal antibodies as tools to study cell wall composition in the *Cuscuta* species. In view of this, the objective is to;

Analyze the presence of Xyloglucan which is a component of hemicellulose. This will assist in detecting and identifying the presence, levels and the locations of the hemicellulose

specific to the parts of *C. platyloba* under investigation and again generate a comprehensive and comparative profiling of cell wall components of the parasites.

2.0 Materials and Methods

2.1 Growth Site and Plant materials

The study was conducted on two *Cuscuta* species; *Cuscuta campestris* and *Cuscuta platyloba*. The parasites were routinely infected on the compatible host plant *Pelargonium zonale* L. in a greenhouse at the Phytotron of the UiT The Arctic University of Norway in 24 h of light exposure at 21°C temperature room.

2.2 Primer Design

To investigate the expression of *Cr-XTH* homologues in *Cuscuta campestris* and *Cuscuta platyloba*, suitable primers were designed using the Primer3 program (<http://frodo.wi.mit.edu/primer3/>) under specified default settings:

Primer length: 18-24bp

Amplicon size: 75-250bp

GC content: 50-60%

Optimal Tm: 60°C (calculated by the Primer3 software)

The OligoAnalyzer tool was used to check for hairpin or hetero-dimers by using the link:

<http://eu.idtdna.com/analyzer/Applications/OligoAnalyzer/default.aspx>. To verify gene specificity, primers were blasted against *C. campestris* and *C. platyloba* EST databases.

Table 2- Primers used to check the expression of *Cr-XTH* homologues in *Cuscuta campestris* (*Cc*) and *Cuscuta platyloba* (*Cp*); *Cr-Cuscuta reflexa*.

Gene Symbol	Gene Name	Sequence 5'- 3'
<i>Cuscuta Campestris</i>		
<i>Cc-XTH1</i>	<i>Xyloglucan endo-transglycosylase/hydrolase</i>	F- TCACCGCCTACTACCGAAAC R- GTTCTTCTGGACCCACCTCA
<i>Cc-XTH2</i>	<i>Xyloglucan endo-transglycosylase/hydrolase</i>	F- TAAGGCCAGATAACCCACAG R- AAACATGAGCCCAATTCCAC
<i>Cc-Actin</i>	<i>Actin 7 (ACT7)</i>	F- GAGTCATCTTCTCACGGTTAGC R- GCAGTCTTCCCTAGCATTGTGG
<i>Cc-EF1α</i>	<i>GTP binding Elongation factor</i>	F- CAAGCGTGTAATTGAGGGGC R- TCAACGTGTGAGGTTCCAGT
<i>Cc-G6PD</i>	<i>Glucose-6-phosphate dehydrogenase 5</i>	F-TCTACCTTGCACCTCCCTCCA R- TTCTCAGCTGTGGCCGAATC
<i>Cc-SF2</i>	<i>SF2/ASF splicing modulator Srp30</i>	F-TGGTTTGTGCGAGGCGTTCTG R-CTACCACTCCAGACATTCCAC
<i>Cuscuta platyloba</i>		
<i>Cp-XTH1</i>	<i>Xyloglucan endo-transglycosylase/hydrolase</i>	F- CAGCAATTCCACCTCTGGTT R- AGATGATGTGTTGGGGCTTC
<i>Cp-XTH2</i>	<i>Xyloglucan endo-transglycosylase/hydrolase</i>	F-ATCTGTTCGGGCATTTCAAC R- TGGGGTCAAACCAGAGGTAG
<i>Cp-Actin</i>	<i>Actin 7 (ACT7)</i>	F- AAGCCCAATCGAAAAGAGGT R- ACATGGCAGGGGTGTTAAAG
<i>Cp-EF1α</i>	<i>GTP binding Elongation factor</i>	F- GGAGTTGTGGCATCCATCTT R- GGTCGACTGTGCTGTTTTGA
<i>Cp-G6PD</i>	<i>Glucose-6-phosphate dehydrogenase 5</i>	F- AGTGCAATTTTGGTCCTTGC R- GGTGCCTCTCCATTGTTGTT
<i>Cp-SF2</i>	<i>SF2/ASF splicing modulator Srp30</i>	F- CTTGATGCGTCTGAGTTCCA R- CCACCACTCTTCCCTCTTGA

2.3 Tissue harvesting and homogenization

Prior to the extraction processes, the cross-sections of infection sites of both *Cuscuta campestris* and *Cuscuta platyloba* on *Pelargonium zonale* L were viewed under the Stereo-Lumar. V12.0 microscope.

For sampling of larger pieces of *Cuscuta* species, the young haustoria (at the initial host attachment stages) and stems from each species were kept in moist-clean papers immediately after harvesting from the host plants.

The harvested samples (young haustoria and stems) were manually extracted with a sharp scalpel and taken in triplicates into differently labelled 2 mL Eppendorf Safe-Lock Tubes and immediately frozen in liquid nitrogen for further analysis. Sampling was done in summer and the weight of each sample was recorded.

During the preparation of sample extracts, 2 tungsten carbide beads of size 3mm were placed into each tube before being ground into a fine powder using a TissueLyser manufactured by QIAGEN. The adapters of the TissueLyser were pre-cooled at -20 °C to avoid thawing of the tissue during disruption. To achieve such fine texture, grinding was repeated twice at the frequency 30.0 (1/s) for 30.0 sec and samples were frozen in Liquid N₂ between each grinding interval. Each homogenised sample was separated into 2; 1 part for the analysis of the expression of *Cr-XTH* homologues in *Cuscuta campestris* and *Cuscuta platyloba* and the other part was used to investigate the activity of XTHs in the same species. Samples were stored at -80°C prior to RNA or protein isolation.

2.3.1 RNA Isolation

Reagents:
β-Mercaptoethanol (β-ME)
Buffer RLT (Guanidine Isothiocyanate)
96% Ethanol, Buffer RW1
Buffer RPE, RNase-free water

Plant Mini Equipment:
RNeasy Mini Spin Columns (pink)
QIAshredder Spin Columns (lilac)
Collection Tubes (2 mL)
Collection Tubes (1.5 mL)
Safe-Lock Eppendorf tubes (1.5 mL)

Total RNA extraction from all the *Cuscuta* species was isolated using the RNeasy Plant Mini Kit (QIAGEN) and the protocol described for RNA isolation from Plant Cells and Tissues and Filamentous Fungi was followed.

QIAshredder spin columns (lilac) and RNeasy spin columns (pink) were labelled with correct *Cuscuta* species, tissue type, number and finally placed in 2-mL collection tubes. For buffer preparation, 60 μ L of β -Mercaptoethanol (β -ME) was added to 6 mL of Buffer RLT (Guanidine Isothiocyanate) in a fume hood and mixed by vortexing for 5 seconds.

Samples were removed from -80°C bio-freezer and immediately chilled in liquid N₂ to prevent thawing. To lyse samples, 450 μ L of lysis buffer containing β -Mercaptoethanol (β -ME) and Buffer RLT was pipetted into each microcentrifuge tube containing \geq 100mg of starting tissue and immediately vortexed vigorously for 3 minutes to disrupt tissues.

The lysate from each species tissue was transferred into each correct labelled QIAshredder spin column (lilac) and centrifuged for 2 minutes at full speed to remove the plant debris. The supernatant of the flow-through from each species tissue was transferred into new 1.5 mL Eppendorf tube and the volume of the filtrates were recorded. Half the volume of 96% ethanol was added to each filtrate and immediately mixed by pipetting.

Each sample was transferred into RNeasy spin column (Pink) and centrifuged for 15seconds/10000 rpm and the flow-through from each sample was discarded. To wash the spin column membrane, 700 μ L of Buffer RW1 was added to each RNeasy spin column, centrifuged and the flow-through was discarded.

Afterwards, 500 μ L of Buffer RPE was added directly to each of the RNeasy spin column (Pink), centrifuged for 15 seconds/ 10000 rpm and the flow-through was discarded. This spin column membrane wash process was repeated once but centrifuged for 2 minutes/ 10000rpm. Another centrifugation was carried for 1 minute at full speed and in 2 mL new collection tubes.

The RNeasy spin columns were placed in 1.5 mL collection tubes, 50 μ L RNeasy-free water was pipetted directly to each spin column membrane and centrifuged 1 minute at 10000 rpm to elute the total RNA from each sample tissue. The eluted RNA solution from each tissue sample was kept on ice to prevent RNA degradation and later stored in -80°C bio-freezer for further analysis.

2.3.2 Nucleic Acid Measurement

To determine the concentration of Total RNA and assess the overall purity of the extracted RNA sample from each species tissue sample, the NanoDrop™ 1000 Spectrophotometer by ThermoFisher Scientific was used and its protocol was followed accordingly. Unlike other methods, the quantification of the amount of the total RNA does not require any dilution of RNA solution. The software to determine the amount of nucleic acid was launched.

Reagents:	Equipment:
RNA samples to be measured	NanoDrop™ 1000c Spectrophotometer
Distilled water	Pipette with tips
Blanking solution: RNase free-water	Lint-free laboratory wipe

The lower and upper pedestals of the NanoDrop were cleaned with distilled water and wiped vigorously with Lint-free laboratory wipe. Initialization of the NanoDrop software was done by pipetting 1 μL of distilled water on the lower pedestal. The pedestals were dried with Lint-free laboratory wipe after NanoDrop initialized. The NanoDrop was blanked by pipetting 1 μL of RNase-free water on the lower pedestal. To measure total RNA in each species sample, 1 μL of the sample was used, the sample type was named, and the various measurement parameters (RNA, ratios-260/280 and 260/280) were adjusted in the software and the concentration ($\text{ng}/\mu\text{L}$) and various absorbance data were recorded. Prior to each measurement, sample was carefully flicked to mixed well and achieved accurate data. Finally, the lower and upper pedestals were cleaned with distilled water and Lint-free laboratory wipe.

2.3.3 DNase Treatment

The removal of genomic DNA from the extracted Total RNA of all the *Cuscuta* species tissue samples were carried out by using DNA-free™ Kit (Ambion) by ThermoFisher Scientific. This method for DNase treatment allowed to effectively remove the contaminated DNA from the RNA samples. From each of the *Cuscuta* species RNA isolates, a 20 μL reaction was set-up for DNase treatment of 2 μg (2000 ng) total RNA.

Reagents:
10× DNase I Buffer
rDNase I (2 Units/ μL)
Total RNA, RNase free Water

Equipment:
Adjustable pipette
1.5 mL Safe-Lock Eppendorf tubes
Eppendorf Thermomixer

The DNase treatment was carried out by preparing a 20 μL reaction set-up for each RNA *Cuscuta* species tissue sample by the addition of the following components in a 1.5 mL tube for each sample.

Table 3- Reaction component for DNase Treatment.

Components	Volume (μL) per tube
10× DNase I Buffer	2
rDNase I (2 Units/ μL)	1
Total RNA	2 μg (2000 ng)
RNase free Water	To 20 final

The content of each sample tube was mixed by gently flicking the tube and incubated in an Eppendorf Thermomixer at 37°C for 30 minutes. Resuspension by vortexing was done after the addition of 2 μL DNase Inactivation Reagent to each tube. The tubes were thoroughly mixed by flicking, incubated at room temperature for 2 minutes but mixed occasionally to redistribute the DNase Inactivation Reagent during the incubation process.

The tubes were centrifuged at $10\,000 \times g$ for 1.5 minutes and each supernatant which contained DNA-free RNA was transferred into each fresh new Safe-Lock Eppendorf tubes. The transfer of the supernatant was successfully achieved by avoiding the transfer of the DNase Inactivation Reagent pellet. The DNase treated samples were kept in -20°C for further treatments. Hence, due to the low concentration of total RNA in some samples, volume adjustment was made for such tissue sample and in certain instance, RNase-free water was not added.

2.3.4 Gel Electrophoresis Analysis

After the total RNA isolation and DNase Treatment of all the *Cuscuta* tissue RNA isolates, agarose gel electrophoresis was conducted to check the purity and integrity of isolated RNA.

Reagents:
<i>Cuscuta</i> tissue samples, 1× TAE Buffer Agarose Powder, Gel Red 6× TriTrack DNA Loading Dye 0.25 µL Gene rule 1Kb
Equipment:
Gel Casting Tray, Gel/well comb, Voltage source, Microwave, Gel Box Microwavable Glass Conical flask, Fume Hood, BIO- RAD ChemiDoc MP Imaging System (UV Light source)

This method involved the preparation and casting of the agarose gel with the appropriate concentration, loading of the samples into each well, connecting the gel to an electric voltage for a period to achieve a maximum separation and finally, visualisation of the gel under UV light.

About 400 ng total RNA was run on a 1% Agarose gel to verify that the isolated RNA and DNase treated samples were intact and free from DNA contamination.

The first stage of the Agarose Gel preparation proceeded by measuring 80 mL of 1× TAE buffer into a microwavable glass conical flask and 0.8 g of the Agarose powder was added onto it and gently shaken to mixed well in the 1× TAE buffer.

The content (i.e. 1× TAE buffer + Agarose powder) was microwaved for 3 minutes, whilst the microwave was pulsed, and flask was swirled occasionally as solution heated up. The melted agarose was slightly cooled down under a cold running tap, 8 µL of Gel red was pipetted to it and gently shaken to mixed well. The Gel Casting Tray was sealed by tightening the ends and balanced with the movable boats beneath. Air-bubbles were prevented from being trapped in the gel by slowly pouring the agarose in the Gel Casting tray and finally the gel comb was inserted. The newly

prepared gel was allowed to stand in a fume hood and under room temperature until it completely solidified.

After the gel solidification, the gel was transferred to a Gel box and appropriate amount of 1× TAE buffer was gently poured into it to completely cover the gel surface and the gel comb was slowly removed from the gel. The *Cuscuta* tissue samples to be loaded into the gel were prepared according to the reaction volume set-up below and 10 µL of the prepared sample was loaded into each well, including 3 µL of 0.25 µL Gene Ruler 1Kb into the first gel well but 15 µL was loaded into the well in the case of *CcS2** because its low concentration.

Table 4- Total reaction volumes (µL) of *Cuscuta* tissue samples used for Gel Electrophoresis Analysis.

Type of <i>Cuscuta</i> Tissue sample	Vol. of samples needed (µL)	Vol. of RNase-free Water (µL)	Vol. of 6× TriTrack DNA Loading Dye (µL)
<i>CcH1</i>	2.3	5.7	2
<i>CcH2</i>	2.7	5.3	2
<i>CcH3</i>	3.4	4.6	2
<i>CcS1</i>	2.8	5.2	2
<i>CcS2*</i>	8.3	4.7	2
<i>CcS3</i>	3.7	4.3	2
<i>CpH1</i>	4.2	5.6	2
<i>CpH2</i>	2.1	5.9	2
<i>CpH3</i>	3.1	4.9	2
<i>CpS1</i>	3.6	4.4	2
<i>CpS2</i>	4.8	3.2	2
<i>CpS3</i>	2.6	5.4	2

The Gel Box was covered and connected to an electric source and allowed to run at 70 V for 1hour. After a successful run, the Gel Box electrodes were disconnected from the electric power and then the gel was carefully removed and transferred into a Bio-Rad UV transilluminator for visualisation and photography of the separated fragments.

2.3.5 Reverse Transcription (RT)

To run a successful Quantitative real-time PCR (qPCR), the single-stranded mRNA containing poly(A) tails *Cuscuta* tissues samples i.e. DNase Treated samples must be reverse transcribed to cDNA (complementary DNA). Invitrogen SuperScript II Reverse Transcriptase of the ThermoFisher Scientific was used to reverse transcribed RNA to cDNA. A 20 μ L reaction was set up in separate 1.5 mL Eppendorf Safe-Lock Tube for each *Cuscuta* tissue sample.

Equipment:	Reagents:
1.5 mL Eppendorf Heating Block	100 μ M Anchored Oligo (dT) ₁₈
1.5 mL Eppendorf Safe-Lock Tubes	10 mM dNTPs, DNA-free RNA
Eppendorf Centrifuge 5417R	5 \times First-Strand Buffer, 0.1 M DTT
Sterile filter pipette tips	RNaseOUT Recombinant Ribonuclease Inhibitor
	SuperScript II Reverse Transcriptase

Reactions were set up for all samples by adding the reagents in the order listed below. At every incubation step, the heating block was pre-heated to the specified temperature.

Table 5- First reaction step for Reverse Transcription.

Reagents	Volume per tube (μ L)
100 μ M Anchored Oligo (dT) ₁₈	1
10 mM dNTPs	1
DNA-free RNA	1 μ g = 10 μ L
RNase-free Water	0 (No Added Water)

The content of each tube was mixed by gently flicking it and centrifuged for 30 seconds. Samples were then incubated in heating block at 65^oC for 5 minutes quickly chilled on ice for 20 seconds and briefly centrifuged. Another set of reagents were added accordingly based on the calculated volumes below.

Table 6- Second reaction step for Reverse Transcription.

Reagents	Volume per tube (µL)
5× First-Strand Buffer	4
0.1 M DTT	2
RNaseOUT Recombinant Ribonuclease Inhibitor	0.5

After complete addition, each sample was again mixed by flicking the tube, briefly centrifuged and incubated at 42°C for 2 minutes. Finally, 1 µL of SuperScript II Reverse Transcriptase was added to each tube, incubated at 42°C for 50 minutes and followed by an inactivation stage for 15 minutes and at 70°C. No-RT samples without SuperScript II Reverse Transcriptase were prepared, where 3 replicates were made for each *Cuscuta* species by mixing both haustoria and stem sample in a tube. This was to verify that the DNase Treatment worked out successfully.

2.3.6 Quantitative real-time PCR (qPCR)

The Quantitative real-time PCR (qPCR) method was adopted to measure the abundance of gene-specific cDNA. Reverse Transcription of all DNase Treated RNA isolates were performed in separate tubes and under different reaction conditions with optimized buffers i.e. The two-step RT-qPCR assay. It was carried out with SsoFast Evergreen Supermix from Bio-Rad as a fluorescence dye to detect double stranded DNA in the samples and 20 µL were set up. Samples were run in technical duplicates and negative controls for each target primer pair with water instead of cDNA were included in all runs. For each *Cuscuta* cDNA tissue sample, 100-fold dilution was prepared only for testing the primer pairs and the reaction content included:

Table 7- 100-fold cDNA Dilution from original samples.

Sample	Vol. used from each cDNA tissue sample (µL)	Vol. of Water (µL) used
<i>Cuscuta campestris</i>	2 µL Haustoria tissue sample + 2 µL Stem tissue sample	396
<i>Cuscuta platyloba</i>	2 µL Haustoria tissue sample + 2 µL Stem tissue sample	396

Equipment:
1.5 mL Safe-Lock Eppendorf tubes Sterile Filter Tips 8-caps Eppendorf RT-PCR strips and sealer CFX96™ Real-Time PCR Detection System (Bio-Rad)
Reagent:
SsoFast EvaGreen Supermix 2.5 µM Forward and Reverse Primers cDNA (10 ⁻²) Dilution Water

Real-time PCR Reaction mastermixes were prepared for each 10⁻² fold-dilution *Cuscuta platyloba* tissue samples, where four reference genes and two specific gene primer pair were tested in each sample after the normalisation of the primer pair concentration and mixing of the specific forward and reverse primer pairs. Also, 10⁻² fold Mastermix dilution for *Cuscuta campestris* tissue samples were prepared to test the target-genes.

Table 8- Real-time PCR Reaction mastermixes of volume, 20 μ L/tube for each *Cuscuta* tissue sample.

Reagents	1 \times MM Reaction set (μ L)	16 \times MM Reaction set (μ L)	8 \times MM Reaction for Negative Controls (μ L)
SsoFast EvaGreen Supermix	10	160	80
2.5 μ M F and R primers	4	-	-
10 ⁻² cDNA Template	5	80	40 ~ H ₂ O
Water	1	16	8

The reactions were assembled on ice, where each of the primer pairs were added into their specific tubes, gently mixed and span down. A pipetting scheme was drawn to direct the pattern. For the amplification and detection of all qPCR reactions, the CFX96 Real-Time PCR Detection System was used and the PCR tubes – reading was done following the program settings below. Finally, the data was analysed with the CFX Manager Software and melt curves were generated.

Table 9- Program set-up for Primer Optimisation.

Steps	Temperature ($^{\circ}$ C)	Time (sec)	No. of cycles
Enzyme activation	95	30	
Denaturation	95	5	40
Annealing/Extension	61	5	
Melt Curve	65-95	5 sec/step	

After a complete program-run, the PCR tubes were removed from the machine and a verification of the PCR specificity and correct sizes during amplification were conducted on 1% Agarose Gel by using 15 μ L reaction which included of 4 μ L 6 \times TriTrack DNA Loading Dye and 3 μ L Gene ruler 1Kb. A UVP Dual-Intensity Transilluminator was used to view the migration of samples and finally, fragments photography of the Agarose Gel was taken under BIO-RAD ChemiDoc MP Imaging System.

2.3.7 Assay Validation

The primer pairs amplification efficiency was determined by using the Standard Curve Method. The standard curve derived from the serial cDNA dilutions determined the efficiency of amplification for each specific primer pairs. With this quantification method, 10-fold serial dilutions of cDNA which ranged from 10^{-1} to 10^{-5} was adopted and the best dilution level of the cDNA that ran through all was chosen for Gene Expression Analysis. In the dilution, 10 μ L of the original sample was mixed 90 μ L of H₂O and the dilution chain continued to 10^{-5} -fold. A mastermix reaction scheme was drawn, where prepared samples were pipetted into a PCR tube according to the specified pipetting pattern drawn and samples were run in CFX96 Real-Time PCR Detection System controlled by a standardized software program and final data were assessed.

Reagents:
SsoFast EvaGreen Supermix
2.5 μ M F and R primer pairs
cDNA (10^{-1} to 10^{-5}) dilution series
Water

Equipment:
CFX96 Real-Time PCR Detection System
1.5 mL Safe-Lock Eppendorf tubes
Sterile Filter Tips
8-caps Eppendorf RT-PCR strips and sealer

Table 10- Reaction setup for Assay Validation Analysis.

Components	1 MM \times Reaction setup (μ L)	19 \times MM Reaction setup (μ L)
SsoFast EvaGreen Supermix	10	190
2.5 μ M F and R primers	4	76
10-2 cDNA Template	5	- (~ H ₂ O)
Water	1	19

Note: The 19 \times Mastermix Reaction setup were prepared separately for each 10-fold dilution series with 20 μ L/tube. All Mastermixes included Negative Control templates.

***19 \times MM = Triplicate of 10-fold dilution templates (15 \times) + 2 \times negative controls + 2 \times additional which accounted for possible pipetting errors.**

2.3.8 Gene Expression Analysis

To determine the expression of the two target genes, *XTH-1* and *XTH-2* and four reference genes, *Actin*, *EF1 α* , *G6PD*, and *SF2* in *Cuscuta campestris* and *Cuscuta platyloba* tissue samples, these six genes were assessed in two-steps RT-qPCR where the $2^{-\Delta\Delta CT}$ (Livak) was adopted in the interpretation of the results. The Assay validation results showed amplification efficiency to be equal and > 99.5% and 100-fold dilution templates were used in the preparation of the Gene Expression Assays (i.e. 3 μ L cDNA + 297 μ L H₂O).

Equipment:	Reagents:
96-Well PCR Plate	SsoFast EvaGreen Supermix
CFX96 Real-Time PCR Detection System	2.5 μ M F and R primers
1.5 mL Safe-Lock Eppendorf tubes	10 ⁻² cDNA Template
	Water

Table 11- Reaction setup for the Gene Expression Analysis.

Components	1 MM \times Reaction setup (μ L)	16 \times MM Reaction setup (μ L)
SsoFast EvaGreen Supermix	10	160
2.5 μ M F and R primers	4	64
10 ⁻² cDNA Template	5	- (~ H ₂ O)
Water	1	16

***15 \times MM = Duplicate of 10-fold dilution templates (12 \times) + 1 \times negative controls + 2 \times additional templates. Inter-run calibrators were included to account for variances between qPCR runs.**

2.4 Quantification of XET Activity in *Cuscuta platyloba* and *Cuscuta campestris*

This experiment was based on two main steps which included the determination of protein concentration and Dot-blot analysis for XET activity.

The protein concentration data were determined by comparing the prepared protein assay with unknown concentration to BSA dilution-series of standards with known concentration. Both protein assay and BSA standards were similarly prepared and under the same condition to aid in results comparison.

Equipment:	Reagents:
1.5 mL Safe-lock Eppendorf tubes	Bovine Serum Albumin
Small-rubber pestle	Deionized (DDI) water
Spectrophotometer	Dye Reagent Concentrate
Whatman #1 filter	<i>Cuscuta</i> tissue samples
Falcon 15 mL Conical Centrifuge Tubes	Sea-sand
1.5 mL Spectrophotometer Cuvettes	
UV Vis Spectrophotometer	

An assay dye reagent was prepared by diluting one part Bio-Rad Dye Reagent Concentrate with four parts distilled deionized (DDI) water. The particles from the resulting solution were removed by filtration through Whatman #1 filter paper. Any unused diluted dye reagent was kept under room temperature for not more than two weeks.

The Bovine Serum Albumin (BSA) standard was reconstituted by adding 20 mL of distilled deionized water and vigorously vortexed to dissolve particulates. The unused sample was aliquoted into 1.5 mL Safe-Lock Eppendorf tubes and kept at -20°C freezer.

A five-step dilution series of BSA stock solution were prepared to create standard curve of the known concentration and linear range of the assay was from 1.0 to 0.2 mg/mL of 100 µL volume. Hence, six 1.5 mL of Eppendorf tubes were labelled, and the following components were added:

Table 12- The Dilution scheme for BSA Standard Assays of volume 100 µL.

Linear Range (mg/mL)	Vol. of BSA Stock (µL)	Vol. of Deionized H ₂ O (µL)
1.0	100	-
0.8	80	20
0.6	60	40
0.4	40	60
0.2	20	80
*H₂O for Blank	-	100

The BSA standard curve was created by pipetting 16 μL of BSA standard solution into 1.5 mL Eppendorf tube and adding 800 μL of the diluted Bio-Rad Dye Reagent Concentrate. The solution was vortexed to be uniformly mixed. The BSA standard samples were incubated for 5 minutes but not more than 1 hour and at room temperature. The absorbance of each BSA solution was measured at 595 nm, with UV Vis Spectrophotometer and in 1.5 mL Spectrophotometer Cuvettes. The sample with water was used to blank the Spectrophotometer.

For the preparation of the enzyme extracts, the sample tissues parts of *Cuscuta campestris* and *Cuscuta platyloba* which was to be investigated were separated into twelve different well-labelled 1.5 mL Eppendorf tubes and a pinch of sea-sand was added to each tube to facilitate the grinding. Using a small-rubber pestle, each sample was ground in ice-cold extraction buffer which constituted 50 mM sodium acetate (pH 5.5), 300 mM NaCl, 20 mM ascorbate, 10 mM CaCl_2 , 15% (v/v) glycerol, 3% (w/v) polyvinylpyrrolidone (PVP-40). Hence, the small-rubber pestles were changed into clean ones when grinding a new *Cuscuta* tissue sample to avoid contamination and 1 mL extraction buffer was used for 200 mg (0.2g) *Cuscuta* tissue sample.

Table 13- Total Weight of *Cuscuta* tissue sample and the volume of ice-cold extraction buffer required.

<i>Cuscuta</i> Tissue Sample	Weight (g) sample	Vol. ice-cold extraction buffer (mL)
<i>Cc</i> H1	0.03	0.15
<i>Cc</i> H2	0.03	0.15
<i>Cc</i> H3	0.01	0.05
<i>Cc</i> S1	0.02	0.10
<i>Cc</i> S2	0.10	0.50
<i>Cc</i> S3	0.11	0.55
<i>Cp</i> H1	0.03	0.15
<i>Cp</i> H2	0.05	0.23
<i>Cp</i> H3	0.05	0.24
<i>Cp</i> S1	0.11	0.55
<i>Cp</i> S2	0.09	0.45
<i>Cp</i> S3	0.08	0.41

After a successful grinding, the homogenates were incubated on ice for 2 hours, centrifuged for 5 minutes at 12 000 g and each resulting supernatant was transferred into fresh new 1.5 mL Eppendorf tube.

The determination of Protein concentration which was the unknown sample was achieved by using Bio-Rad Protein Assay protocol, where 8 μ L of Enzyme or protein extract, 8 μ L of deionized H₂O and 800 μ L of diluted Bio-Rad dye reagent were pipetted into 1.5 mL Eppendorf tube and vortexed to be completely mixed well. Following the same procedure of the BSA Spectrophotometer measurement, absorbance measurements were conducted, and results were recorded. Prior to that, 100 μ L of each standard and sample solution were pipetted into clean tubes. The linear range of 0.2 to 1.5 mg/mL was used to get the range within the standard curve range.

A graph of standard curve was generated by plotting the absorbance (595 nm) on the y-axis and the concentration of the BSA standards on the x-axis by using Microsoft Excel. Since the concentration of protein was unknown, they could not be graphed on the standard curve; rather, a linear regression to fit the results were performed. The regression equation was used to calculate the values of the unknown Protein concentration.

2.4.1 Xyloglucan Endotransglucosylase (XET) Dot Blot Analysis

To detect the presence and relative activity of XET's in the *Cuscuta campestris* and *Cuscuta platyloba* tissue samples which were under investigation, the novel Dot Blot method by (Fry 1997) was adopted. This experimental procedure involved the preparation of XyGO-SR, XET test paper, enzyme extracts, loading of tissue extracts on test papers and imaging with ChemiDoc MP Imaging System (Bio-Rad).

Reagents:
Xyloglucan, XyGO-SR
Enzyme Extracts, Distilled Water
Ethanol: Formic Acid: Water (1:1:1)

Equipment:
Whatman #1 Filter Papers
Acetate Envelope
Rotating Shaker
ChemiDoc MP Imaging System (Bio-Rad).

The preparation of Xyloglucan, XyGO-SR and Dot Blot assay were carried out as described in Fry,1997. XET test papers were coated with Xyloglucan and XyGO-SR and one control paper, prepared by coating with Xyloglucan but without XyGO-SR. Already prepared *Cuscuta* enzyme extracts (3 μ L volume) were loaded unto XET test papers at cold room and 1hour incubation in acetate envelope at dark area at room temperature.

Prior to the loading, the XET test papers were grid and labelled with pencil, where the last end of the paper was marked “BLANK”. Hence, labelling assisted in the location of individual enzyme extract in the right grid. In Ethanol: Formic Acid: Water (1:1:1), the background of the XET test papers were de-stained by 24 hours washing with gentle continuous agitation on a rotating shaker, followed by rinsing in distilled water and then allowed to dry up.

Fluorescent images of the dried XET test papers were taken with ChemiDoc MP Imaging System (Bio-Rad) and by applying the Cy3 application with 400 ms exposure time. Finally, using the global background adjustment volumes, the overall relative levels of XET activity were calculated.

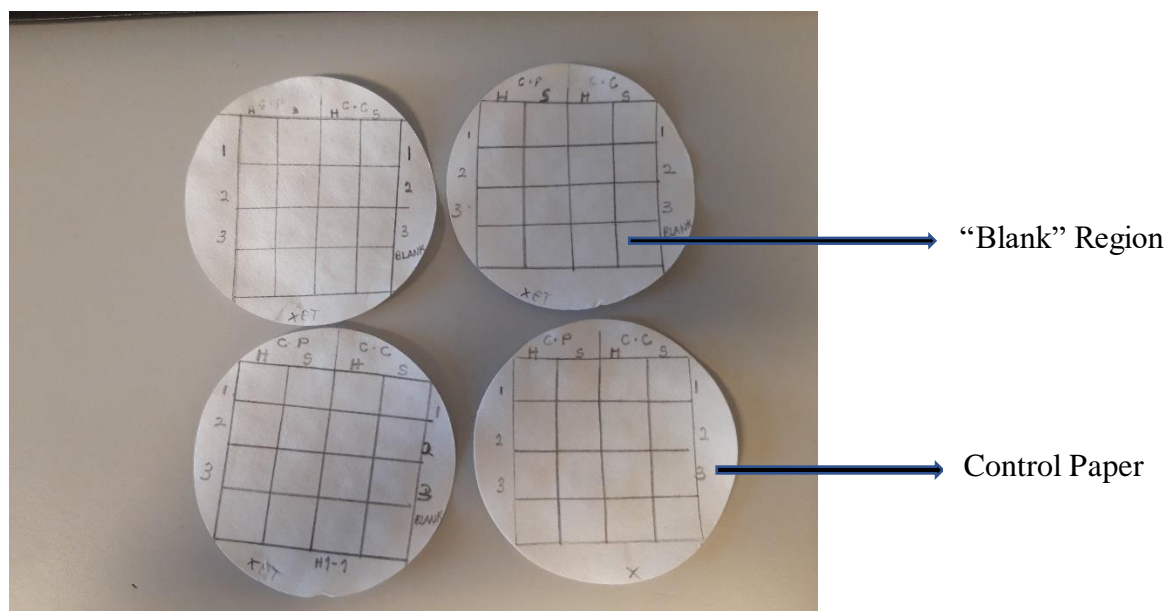


Figure 4- Labelled regions of the XET Test papers which guided blotting pattern.

2.5 Analysing the effect of Coomassie Brilliant Blue R250 on host *Cuscuta* infection

This experimental set-up involved coating the host petioles with Coomassie dye and *Cuscuta platyloba* was infected on the host. The protocol in (Olsen and Krause 2017) was applied in reagent preparation and coating of petioles of the host, *Pelargonium zonale*.

Reagents:	Equipment/materials:
0.005% Poly-L-lysine	Petioles of <i>Pelargonium zonale</i>
5mM Coomassie Brilliant Blue R250	Stem Tissues of parasite, Water Reservoirs
Tap Water	15 mL Falcon Conical Tubes
	Far-red light system, Stereo Lumar V12 microscope with AxioCam MRc5 camera

In preparing the coating dyes, a 15 mL Falcon Conical Tube was filled with a mixture of 0.005% Poly-L-lysine and 5mM Coomassie Brilliant Blue R250 and another with 0.005% Poly-L-lysine which served as the negative control reagent. The petioles of *P. zonale* of the length approximately 10 cm were detached, where 11 set of the detached petioles were submerged the first reagent and another 11 set into the negative control reagent.

The coated petioles were allowed to dry up but to improve the adhesion to the petiole's surfaces, coating was repeated three times interval. The basal section of 1 mm of the coated petioles were cut off to facilitate water uptake and the petioles were placed in water reservoirs. Apical stem tips of *Cuscuta platyloba* were positioned in right angle at close proximity to the host petioles to promote twinning around the host. The growth of haustoria were increased by keeping the set ups under continuous far-red light irradiation for 24 hours day and night regime.

After 12 days, all haustoria were examined by making cross-sections that were viewed under the Stereo Lumar V12 microscope. Images were generated using AxioCam MRc5 camera.

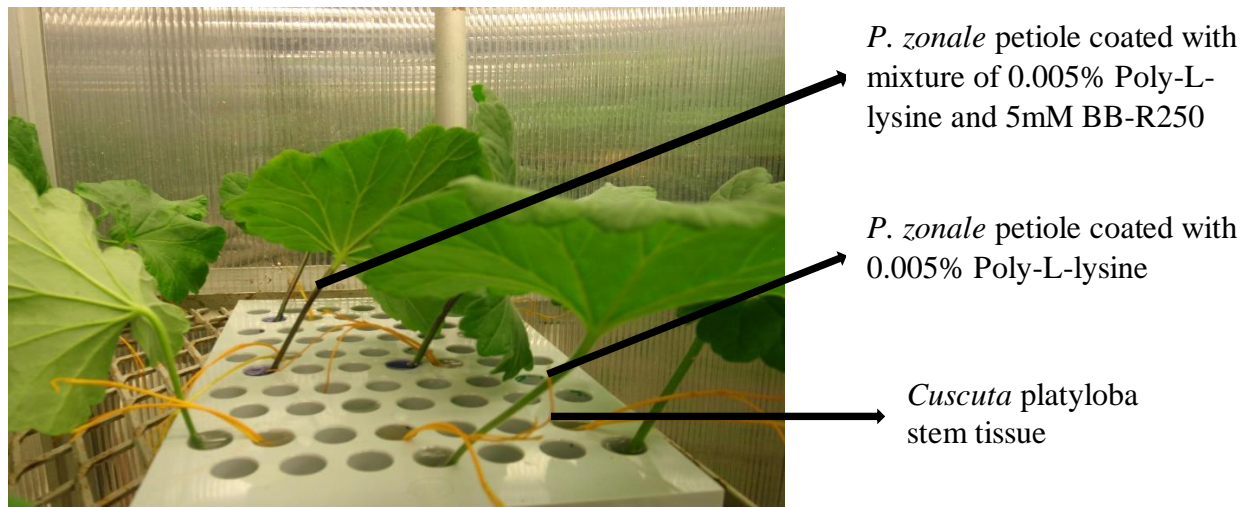


Figure 5- Experimental set up of coated *Cuscuta* petioles tissues.

2.6 Cell Wall polysaccharides Analysis of *Cuscuta platyloba*

In this study, the most common monoclonal antibody that binds to specific xyloglucan hemicellulose of the *Cuscuta* haustoria and stem tissues was selected. These included monoclonal antibody to Xyloglucan (LM25) (Pedersen et al. 2012), for *Cuscuta* haustoria tissue and monoclonal antibody to LM25 for its stem tissue. The LM25 monoclonal antibody binds to the epitope of Xyloglucan. Hence, tissue harvesting, and its homogenisation followed the previously explained procedure in *section 2.3*.

2.6.1 ELISA- Enzyme-linked immunosorbent assay of *Cuscuta platyloba*

The detection of xyloglucan epitope was performed by undergoing through the stages below. In this section, the data which will be used in the analysis will evolve from the ELISA technique stage and this leads to measurement of the relative amount of specific monoclonal antibody against *C. platyloba* extracted from the haustoria and stem sections. The chosen monoclonal antibody has different specificity to hemicellulose but different detection ranges.

Equipment:	Reagents:
Tissue Lyser (Qiagen), Fume hood, Aluminium foil 2 mL Eppendorf Safe-locked tubes and Qiagen tubes 96-Well plate, Pipette with 10 to 12 tips, Rocker	EtOH 70%, 80%, 90% and 100% 100% Acetone, 2:3 Methanol to Chloroform ×1 PBS, 5% Milk powder Specified Primary and Anti-rat (HRP) Deionised Water, Sodium Acetate buffer, 3,3,5,5-TMB in DMSO, 30% v/v hydrogen peroxide, Sulphur Acid

At the AIR preparation (Alcohol Insoluble Residue) stage, the homogenised *Cuscuta platyloba* tissue samples were filled with 1 mL 70% EtOH and rocked for 1 hour. The reagent was pipetted out after centrifuging for 2 min at 4°C/ 14 000 rpm. Aliquots of 1 mL of 80% EtOH were added into each tube and allowed to rock for 1 hour. The same procedures were repeated when 90% EtOH, 100% EtOH, 100% acetone and methanol chloroform (2:3) were sequentially added.

Hence, after the addition of methanol chloroform (2:3), the samples were allowed to shake on rocker for an hour, 1 mL of the reagent was removed and allowed to air-dry under the fume hood overnight. Samples were kept in aluminium foil at room temperature for a period before proceeding to the cell wall extraction stage.

The cell wall extraction stage was carried out by first weighing 1 mg of the AIR *Cuscuta* samples into 2 mL Qiagen tubes, where 400 µL of 4M KOH was added into each tube. In tissue lyser (Qiagen), the prepared samples were ground for 20 minutes. The samples were centrifuged for 15 minutes at 25 000 rpm, supernatants were pipetted out and transferred into new tubes for ELISA. The KOH (diluted, 10-fold in x1 PBS) samples were neutralised with 80% acetic acid.

The final stage of the cell wall component analysis was the ELISA. In this process, six 96-well microtiter plates were labelled with specified *Cuscuta platyloba* tissue sample name and the antibody type to be tested. The basic procedure in ELISA included Coating, Blocking, Detection with primary and secondary antibodies, substrate addition and signal detection.

In each 96-well microtiter plate, 100 μL of $\times 1$ PBS was pipetted into each well, excluding the top row. With the *Cuscuta platyloba* samples, 125 μL of this mixture was pipetted into the top row of each 96-well plate. To make 1:5 titration steps in each plate, 25 μL of the mixture in the first row was pipetted down each row of the plate excluding the bottom row. There, this must only contain $1 \times$ PBS and it served as the negative control and thoroughly mixed by pipetting up and down six times per row. The individual plates were assembled together and incubated on table overnight. After the overnight incubation, blocking and detection stages followed.

Prior to the above mentioned stages, the coating samples were removed by tipping the liquid out and washed out from the plates by vigorously shaking each plate six times under tap water. However, the remaining coating solution was removed by patting the plate on paper towel to dry the plates. At room temperature, 300 μL per well of 5% milk powder in $\times 1$ PBS was pipetted to block the plates. The plates were covered with aluminium foil, incubated for 2 hours, washed and patted as described above.

At the detection stage, a solution buffer was prepared from 5% milk powder and $\times 1$ PBS in the above mentioned monoclonal antibodies and 100 μL of 1:10 dilution was pipetted per well. An hour incubation and $9 \times$ wash with tap water were carried out as described previously. 35 μL of anti-rat antibody coupled with HRP (horse radish peroxidase) was added to (1:1,000 dilution) a mixture of 5% milk powder and $1 \times$ PBS and allowed to stand for 1 hour. Each plate was incubated with 100 μL per well and $9 \times$ wash was carried out. Substrate solution was prepared for each plate containing (9 mL dH_2O , 1 mL sodium acetate, 100 μL (Tetramethylbenzidine) TMB-3,3,5,5 and 10 μL of 6% H_2O_2). Each well of the plate was filled with 100 μL substrate solution and allowed to stand for 8 minutes before the addition of 50 μL 2M sulphuric acid per well. Sulphuric acid stopped the reaction and turned the blue coloured solution to yellow, which signified stable reaction. The absorbance (optical density was read at 450nm) of the plates were read with photospectrometer and results were recorded.

3.0 Results

3.1 The expression of *Cr-XTH* homologues in *Cuscuta campestris* and *Cuscuta platyloba*

Cuscuta campestris and *Cuscuta platyloba* were grown on the host plant, *Pelargonium zonale* and under the same growth conditions, where the haustoria and stem tissue were harvested (section 2.3). Prior to gene expression analysis, RNA was isolated where the first three replicates were selected to proceed with DNase treatments of the RNA isolates and reverse transcription analysis.

The integrity of all the extracts were assessed by running agarose gel electrophoresis as described in the section 2.3.4. All treatments were collected in at least triplicates for each *Cuscuta* tissue sample and hence, the varying concentration and purity of the RNA isolates were checked on the NanoDrop Spectrophotometer (section 2.3.2). Distinct ribosomal RNA bands were achieved from the isolation which indicated high quality (Figure 6).

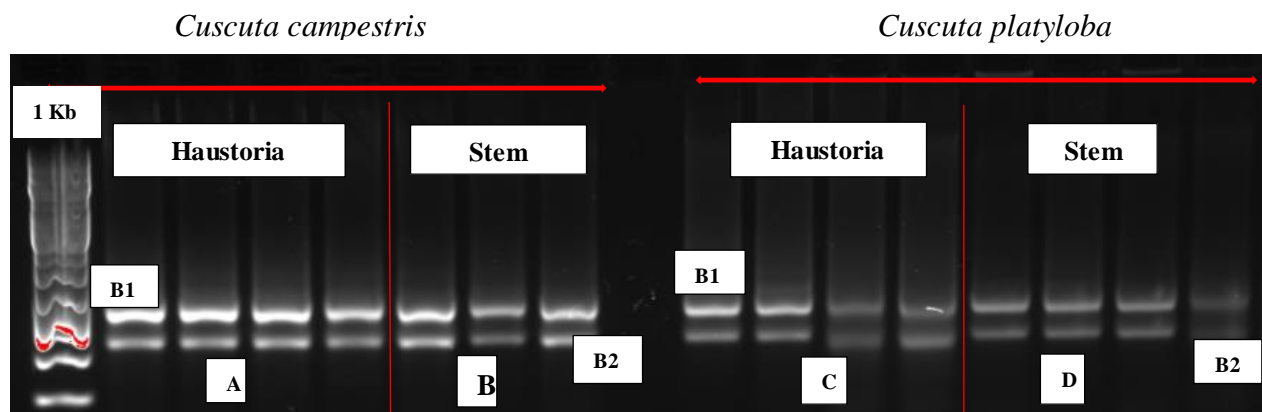


Figure 6- Assessment of the quality of total RNA in *C. campestris* and *C. platyloba*. (A) *Cuscuta campestris* haustoria samples (B) *Cuscuta campestris* stem samples (C) *Cuscuta platyloba* haustoria samples (D) *Cuscuta platyloba* stem samples. The size estimation was achieved by comparing band separation to GeneRuler 1 Kb Ladder. Data from the bands showed the large and small ribosomal subunits (28S and 18S) which are labelled as B1 and B2 respectively. These results represented high quality of isolates without smears. The concentrations of total RNA were used in the calculation of template amount for the cDNA synthesis as shown in appendix II.

3.2 RT-qPCR analysis of *Cr-XTH* homologue in *C. campestris* and *C. platyloba*.

The expression levels of the genes *XTH1* and *XTH2* from the *Cuscuta* species were studied by RT-qPCR by following the protocol described in *section 2.3.6* and using the primers enlisted in *Table 2*. In the analysis, the normalization of the gene was set by using four reference genes also mentioned earlier. Therefore, the samples concentration of cDNA was optimised for the amplification of each gene.

Due to uncertainties about the specificities and amplification efficiencies of the primer pairs, several sets of primer pairs were designed for *Cuscuta platyloba* cDNA samples. These included the same gene type and name but different sequences which were tested and primer pairs with the best results (*Table 2*) were selected for qPCR analysis. Hence, the amplicons ran on the gel verified the expected sizes and that amplicons only have one product (i.e. the latter can also be seen from the melt curve).

Based on the initial technical tests (melt curves, agarose gel electrophoresis and standard curves), six tested primer pairs were selected for gene expression analysis in *C. platyloba* tissue samples and two tested target genes for *C. campestris* tissues samples. However, the other four-reference gene (*Cc-Actin*, *Cc-EF1 α* , *Cc-G6PD* and *Cc-SF2*) designed for *Cuscuta campestris* cDNA samples have been proven in the laboratory to be effective but the two target-genes (*Cc-XTH1* and *Cc-XTH2*) underwent qPCR specific-primer check. Therefore, eight melt curves are represented in the results below (*Figure 7*).

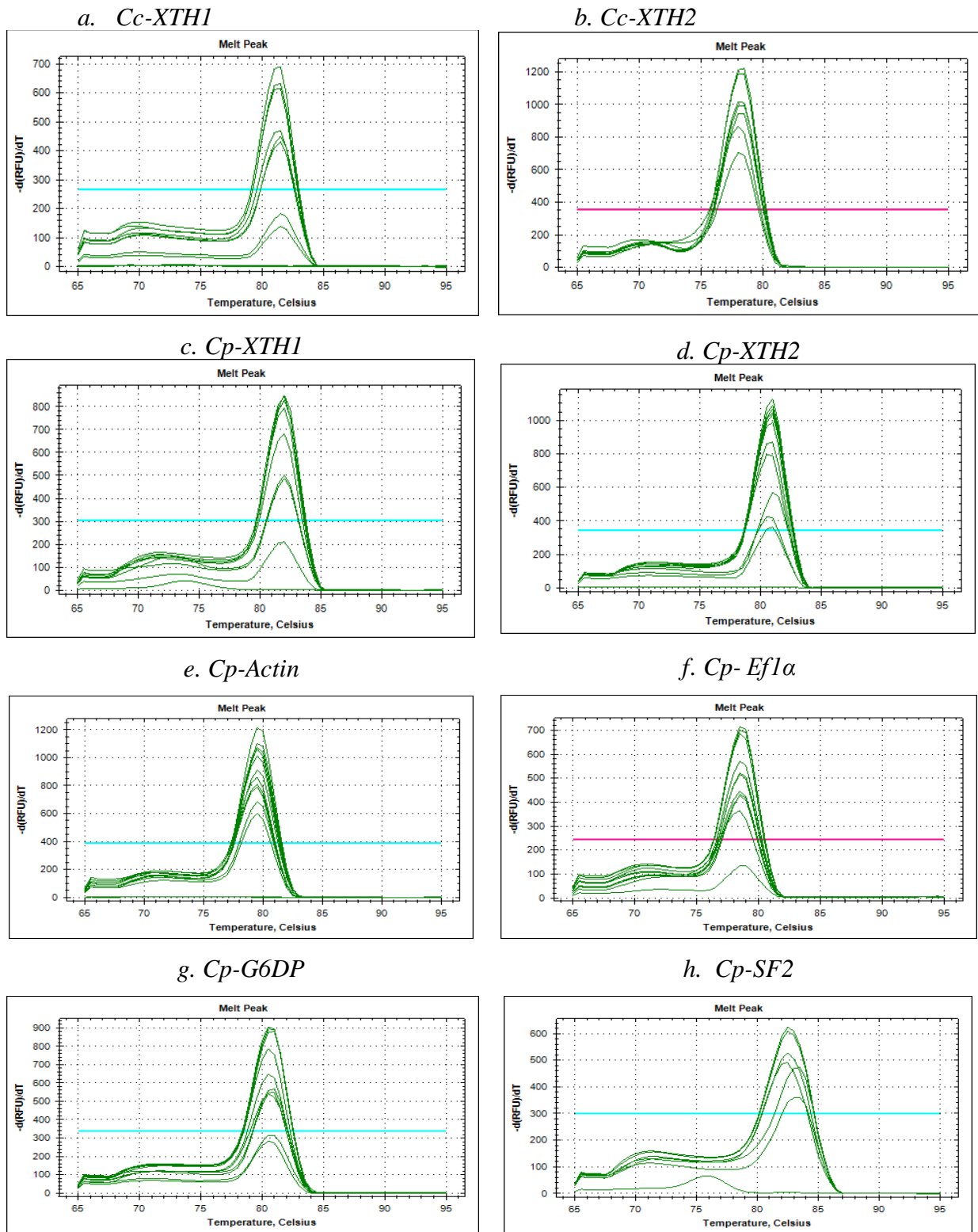


Figure 7- Melt peaks of RT-qPCR amplicons. Letter (a) to (b) depicted the target genes of *Cr-XTH-1* and *Cr-XTH-2* for *Cuscuta campestris* haustoria and stem samples while (c) to (d) and (e) to (h) showed the target and reference genes of *Cuscuta platyloba* haustoria and stem samples respectively. The y-axis represents the negative derivative, $-d(\text{RFU})/dT$ of change in florescence intensities graphed against a

function of temperature in Celsius. The genes *Cp-XTH1* and *Cp-SF2* showed very small melt curves which explain peaks with lower melting temperatures (**Primer dimers**). The melt curves have proven that the tested genes are specific and therefore their final output in the other analysis are expected to yield good results.

3.3 Primer Efficiencies

Serial dilutions of cDNA samples were prepared as showed in *section 2.3.7* to develop the relative standard curves. From the standard curves, efficiencies (E) of the PCR were generated from the formula; $E=10^{-1/\text{slope}}$, where the percentage efficiency was derived from the standard equation as % Efficiency = (E-1) *100%. The respective standard curve results are shown in *Table 14*.

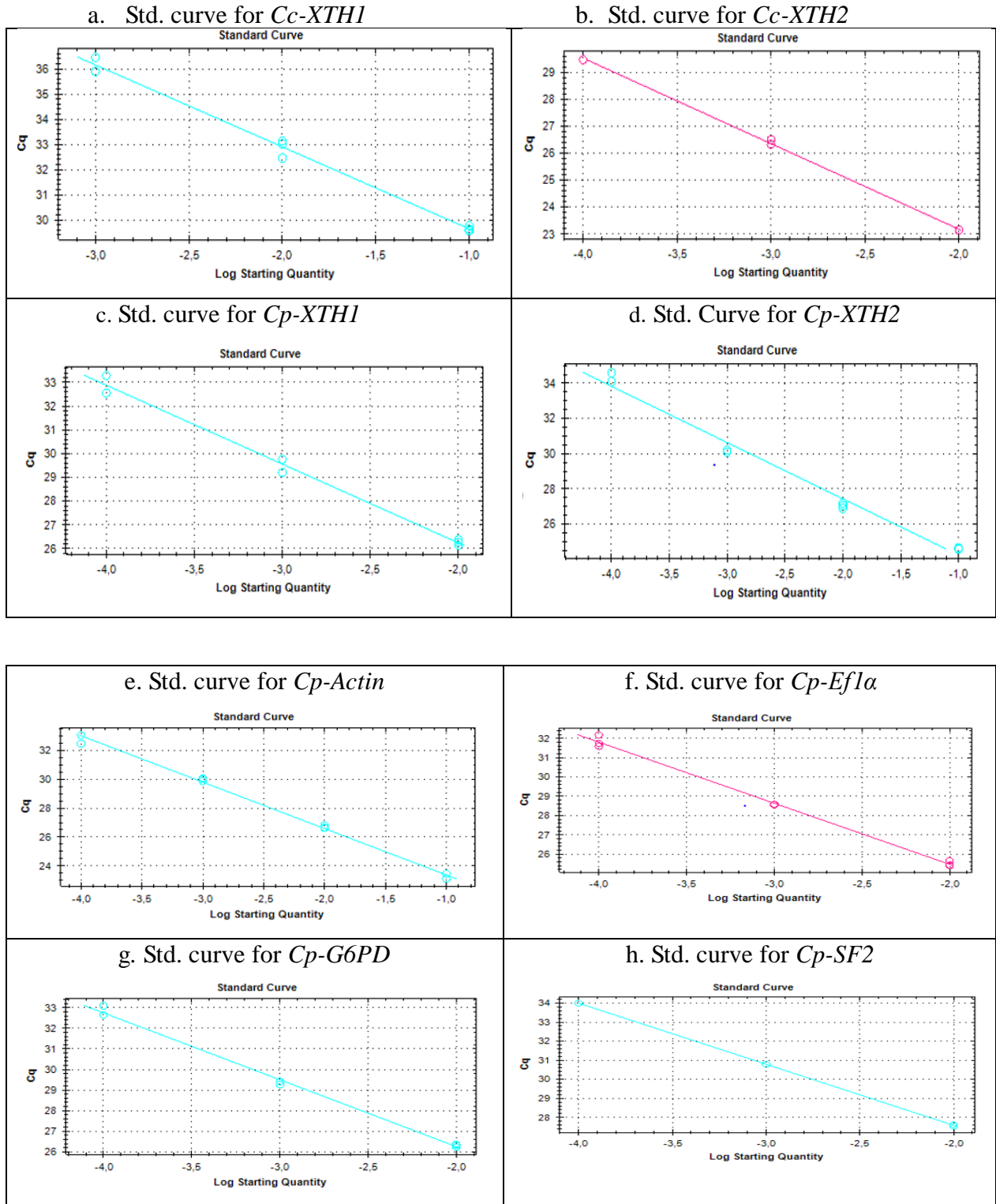


Figure 8- The standard curves for all tested genes. These were generated by amplifying 10,100, 1000-folds serial dilutions of the starting cDNA template. The assay dilutions were run in triplicates. From y-axis of each graph, the respective Cqs were plotted against the log of the starting quantity of each dilution template. The amplification curves from the dilution series were evenly spaced, which depicted consistency across all the reaction replicates.

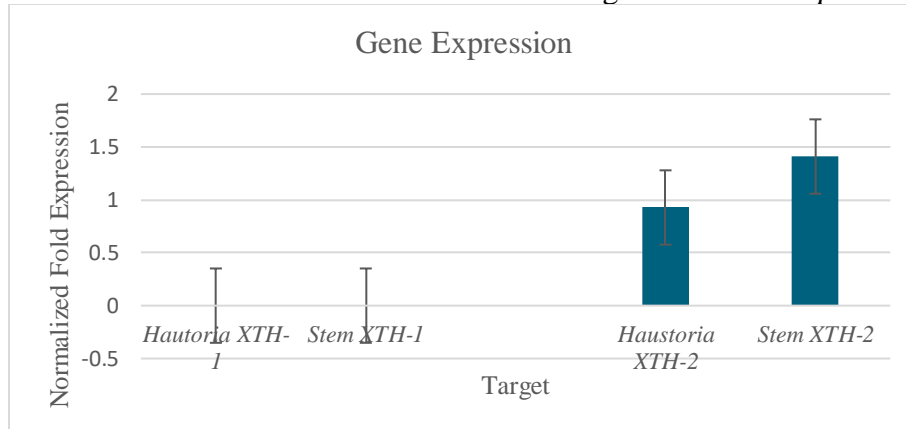
Table 14- The efficiencies of PCR calculated from the respective standard curves. The coefficient of determination (R²) shows the data is accurately described by the regression line. For optimal R², it should be equal to 1 and the percentage amplification efficiencies calculated from the slope of the standard curves were good.

Target	Slope	% PCR Efficiency (%)	R ²
<i>Cc XTH-1</i>	-3.257	102.8	0.991
<i>Cc XTH-2</i>	-3.171	106.7	0.999
<i>Cp XTH-1</i>	-3.321	100.0	0.991
<i>Cp XTH-2</i>	-3.195	105.6	0.984
<i>Cp Actin</i>	-3.206	105.1	0.995
<i>Cp EF1α</i>	-3.170	106.8	0.996
<i>Cp G6PD</i>	-3.251	103.1	0.997
<i>Cp SF2</i>	-3.206	105.1	1.000

3.4 Gene Expression of *XTH-1* and *XTH-2* in *Cuscuta campestris* and *Cuscuta platyloba*

Gene expression analyses were conducted in the haustoria and stem tissues of the *C. campestris* and *C. platyloba*. The quantification of the target genes, *XTH1* and *XTH2* in the selected parts of the *Cuscuta* tissue samples were normalised against all reference genes (*Actin*, *EF1 α* , *G6PD* and *SF2*), followed by the normalisation against each reference gene separately. This was carried out to compensate for differences in the amount of the *Cuscuta* tissue sample used in the studies and further prove the efficiency of the results. The relative expression analysis was determined using 2^{- $\Delta\Delta C_T$} (Livak) method. The expression of the target genes increased or decreased significantly relative to the specific *Cuscuta* tissues analysed.

a. Normalisation with all four reference genes for *C. campestris*



b. Normalisation with all reference gene for *C. platyloba*

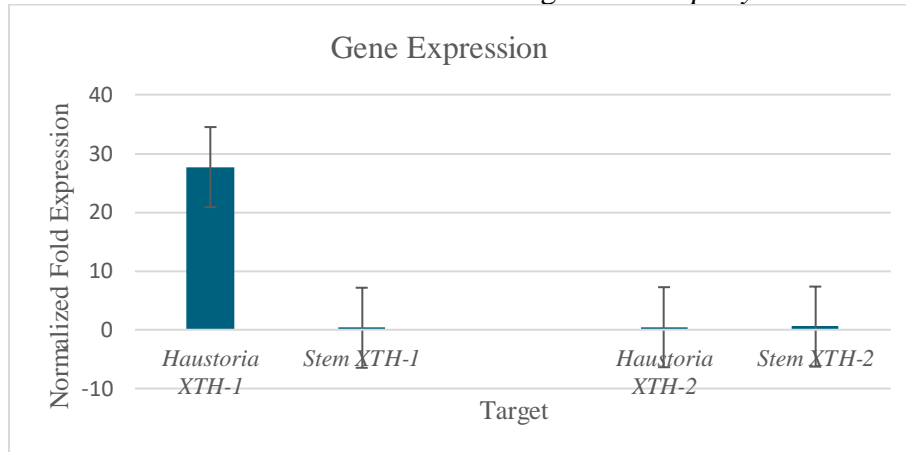


Figure 9- The expression level of gene *XTH1* and *XTH2* from *C. campestris* and *C. platyloba* against the normalisation of all the four reference genes. From the gene expression results, the normalised fold expression on the y-axis was plotted against target. Error bars represent the standard deviation for technical replicates and expression levels showed in three biological replicates. Inter-run calibration for *C. campestris* was run between *XTH2* H1 and *XTH2* H2, *EF1α* H2 and *EF1α* H3 and finally, *Actin* H2 and *Actin* H3. For *C. platyloba*, an inter-run calibration was repeated between H1 and H3 for both the target genes and all the reference genes to improve the successfulness of the analysis. After the normalisation of the reference genes in each *Cuscuta* sample, *XTH2* was upregulated in both the haustoria and stem samples of *C. campestris*. The expression of *XTH2* was higher in the stem than in the haustoria sample of the *C. campestris*. There was no expression of *XTH1* in neither the haustoria nor stem samples of *C. campestris*. Moreover, *XTH1* was highly regulated in the haustoria sample of *C. platyloba* but no signs of expression in the stem sample. The target gene *XTH-2* was very low in both the haustoria and stem samples of *C. platyloba*.

3.5 The Activity levels of xyloglucan endotransglucosylases from *C. campestris* and *C. platyloba*.

3.5.1 The Bovine Serum Albumin (BSA) standards and regression equation

This section generally shows the results of protein concentrations with respect to the standard of measurement which is the Bovine Serum Albumin (BSA). This result enables us to correlate the protein concentration to the unknown standard of measurement. In spite of that, the prepared BSA solution helped to create the standard curve for the protein quantification assay. Also, further understanding about the activity per mg of tissue sample and activity per the protein concentration can be drawn from the analysis through their normalisation.

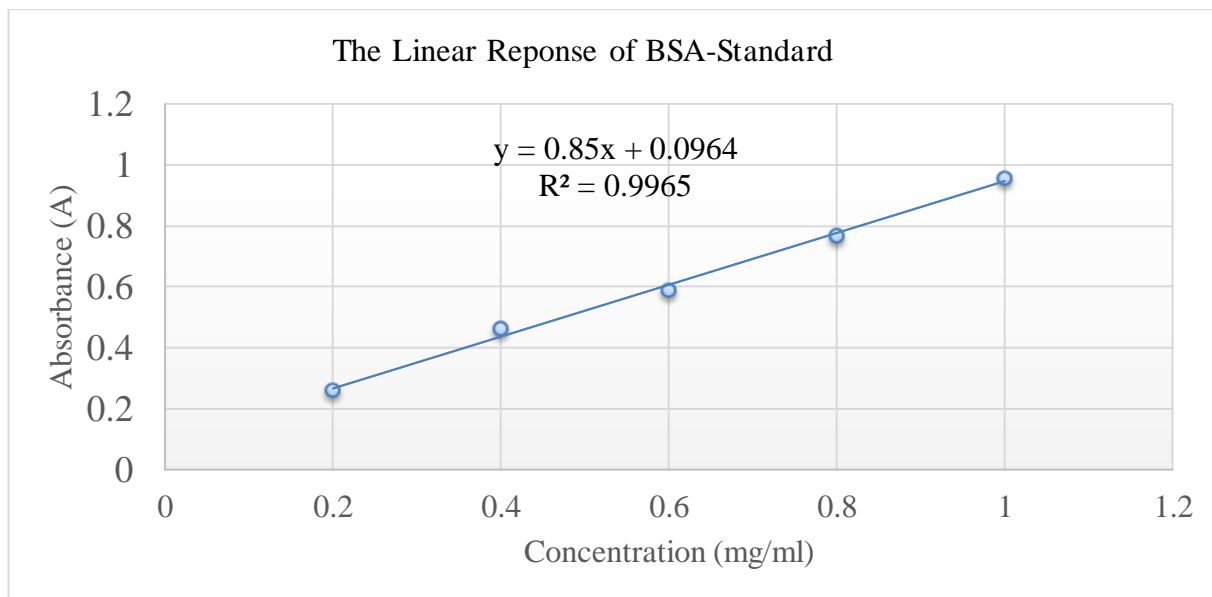


Figure 10- Graphical Representation of Bovine Serum Albumin (BSA) standards. The quantity measurement as absorbance (A) of the BSA assay with known concentration graphed on the y-axis and the concentration (mg/ml) on x-axis (**Hence: the standard for comparison**). Data analysed by fitting Trendlines through the dot series and generating regression equation (R) as “ $y=0.85x + 0.0964$ ”. The unknown concentration (mg/ml) of protein extracts from *C. platyloba* and *C. campestris* tissue samples were determined by intersecting the values of the protein extracts as the values of “x”.

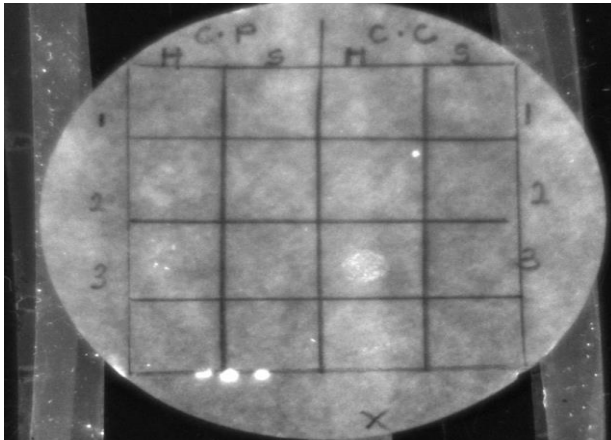
Table 15- The quantitative estimation of the amount of protein extracts present in the unknown solution of *C. platyloba* and *C. campestris* tissue samples. The regression equation generated from the standard of comparison was used to determine the concentration (mg/ml) of the unknown protein extracts.

<i>Cuscuta</i> Sample Names	Absorbance (A)	Concentration (mg/ml)
<i>Cp</i> H1	0.831	1.6055
<i>Cp</i> H2	0.705	1.3913
<i>Cp</i> H3	0.845	1.6293
<i>Cp</i> S1	0.395	0.8643
<i>Cp</i> S2	0.218	0.5634
<i>Cp</i> S3	0.373	0.8269
<i>Cc</i> H1	0.818	1.5834
<i>Cc</i> H2	0.813	1.5749
<i>Cc</i> H3	0.711	1.4015
<i>Cc</i> S1	0.321	0.7385
<i>Cc</i> S2	0.308	0.7164
<i>Cc</i> S3	0.319	0.7351

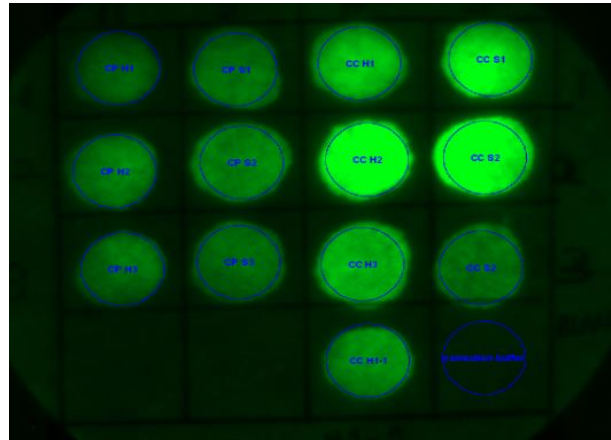
3.5.2 XET activity in *C. platyloba* and *C. campestris* during *P. zonale* infection

To carry out a systematic study on the XET activity, respective spots on the XET test papers were analysed based on the use of the degree of fluorescence and accuracy was ensured by performing technical replicates. The activities of four protein extracts (that is: protein extracts from *C. platyloba* and *C. campestris*) were compared towards the standard set of substrate polymer known as xyloglucan. The XET activity profile from all the replicates are accumulated and various comparisons are made in linearity to the specific region of the *Cuscuta* species under study.

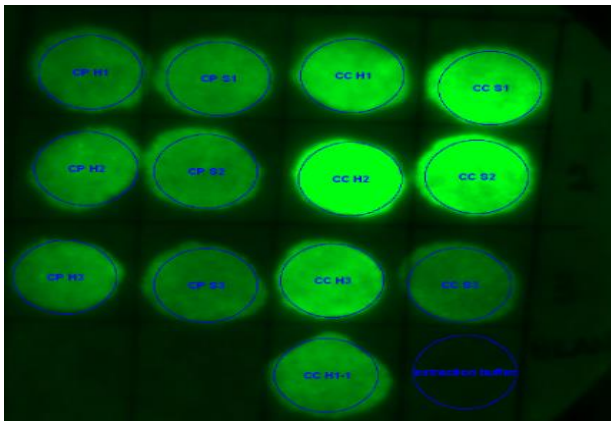
a. XET test paper without XyGO-SR (control)



b. XET test paper with XyGO-SR (Replicate I)



c. XET test paper with XyGO-SR (Replicate II)



d. XET test paper with XyGO-SR (Replicate III)

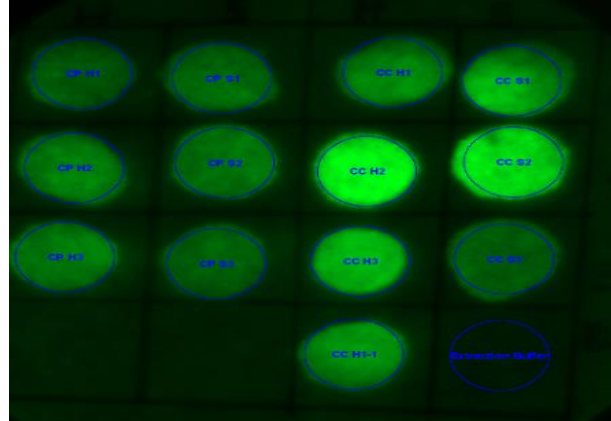


Figure 11- Comparison of the level of XET activity of the haustorium and stem in *C. platyloba* and *C. campestris*. From (a)-(d) depicted the various figures of enzyme extracts; where (a)- showed XET paper without XyGO-SR and (b) to (c)- the three biological replicates for the treatments coated in XyGO-SR. Statistically significant differences between the two treatments (*C. platyloba* and *C. campestris*) with different tissue samples were calculated by two-ways anova and indicated by different letters. Empty circles without any fluorescence indicate the activity levels of the “*extraction buffer*” which basically show no activity and “*CcHI-1*” indicated extra tissue sample included in the analysis.

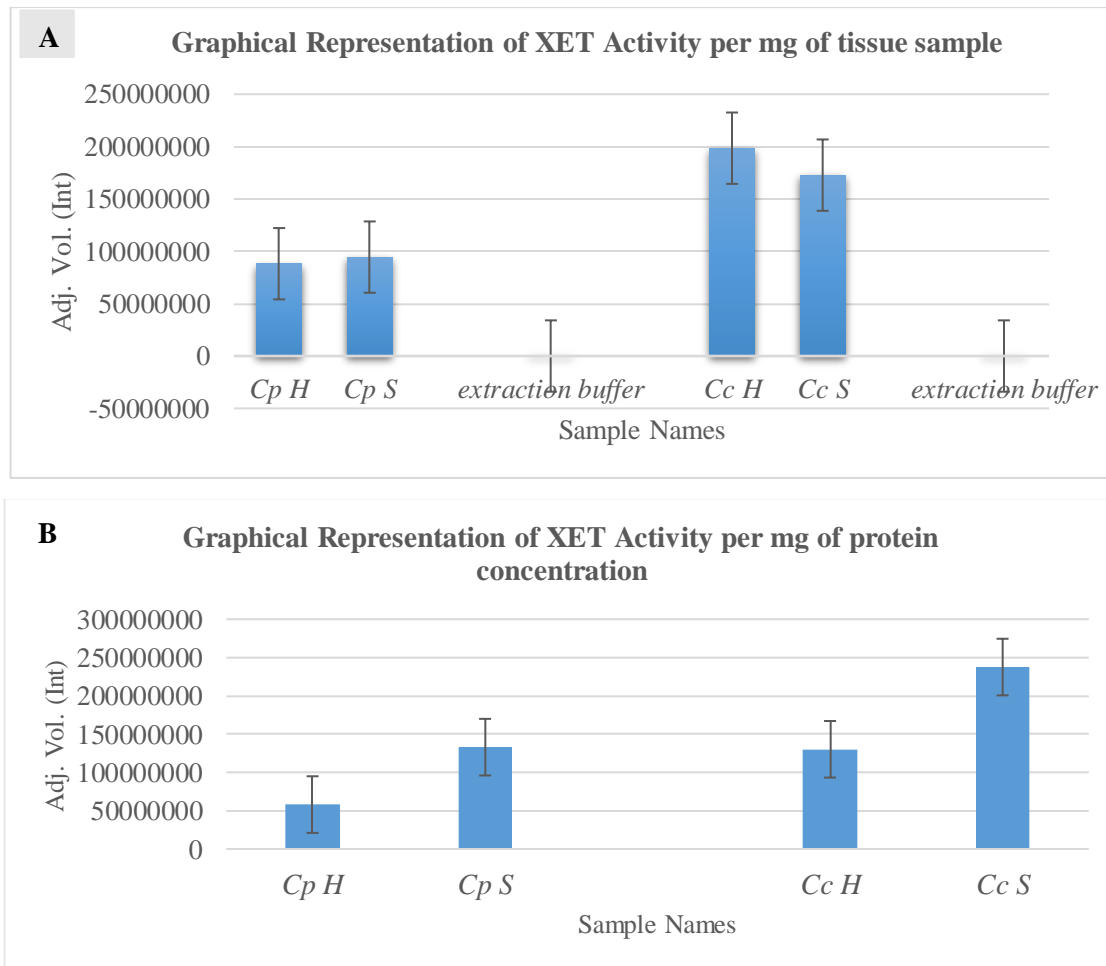


Figure 12- Bar Graph representation of XET Activity in *C. platyloba* and *C. campestris*. Average Dot-blot screens for XET activity in total extracts from the haustoria and stem tissue samples of each *Cuscuta* species (that is: **(A)** activity per mg of tissue sample and **(B)** activity per mg of protein concentration respectively). The extraction buffer shows the control assays. Changes of XET Activity in *C. platyloba* and *C. campestris* haustoria and stem samples, there was approximately equal levels of XET Activity in the haustoria and stem of *C. platyloba* but relatively higher presence of XET in *C. campestris* haustoria than in the stem per mg of tissue sample.

Table 16- Mean separation was completed using Tukeys procedure ($\alpha=0.05$). Cc H and Cc S represent *Cuscuta campestris* haustoria and stem samples whilst Cp H and Cp S also represent *Cuscuta platyloba* haustoria and stem respectively. Means in a column with the same letters are not significantly different from each other. By normalizing per mg (milligram) of protein concentration, showed no significant differences within and between the tissue samples. The table showed significance between the *Cuscuta* samples and vice versa within each *Cuscuta* sample per mg of tissue sample.

A.

Treatment	Mean Adj. Vol
<i>Cc H</i>	198444427 a
<i>Cc S</i>	172721326 a
<i>Cp H</i>	88124355 b
<i>Cp S</i>	94463616 b
ANOVA	P=0.002

B.

Treatment	Per mg of Protein Concentration
<i>Cc H</i>	130163393a
<i>Cc S</i>	237534225a
<i>Cp H</i>	57952347a
<i>Cp S</i>	132950469a
ANOVA	P=0.077

3.6 The parasitization of *Pelargonium zonale* coated with BB-R250 and control

The observation of effect of BB-R250 and control on *P. zonale* petioles was carried out during an experimental set-up described in *section 2.5* by infecting with *C. platyloba*. From **figure 13 a** and **b**, the dark-blue colour represents the BB-R250 inhibitor, whereas **figure 14a** shows the Poly-L-Lysine coated on the petioles of the *P. zonale*. The infusion action in the petioles without BB-R250 are classified as the control in the experiment. After 12 days, successful infections were scored by making cross-sections of about 3mm through all haustoria at their points of attachment to the petioles and viewing them under stereomicroscope. Again, the impeded frequency of *C. platyloba* infections on coated *P. zonale* petioles were tabulated.

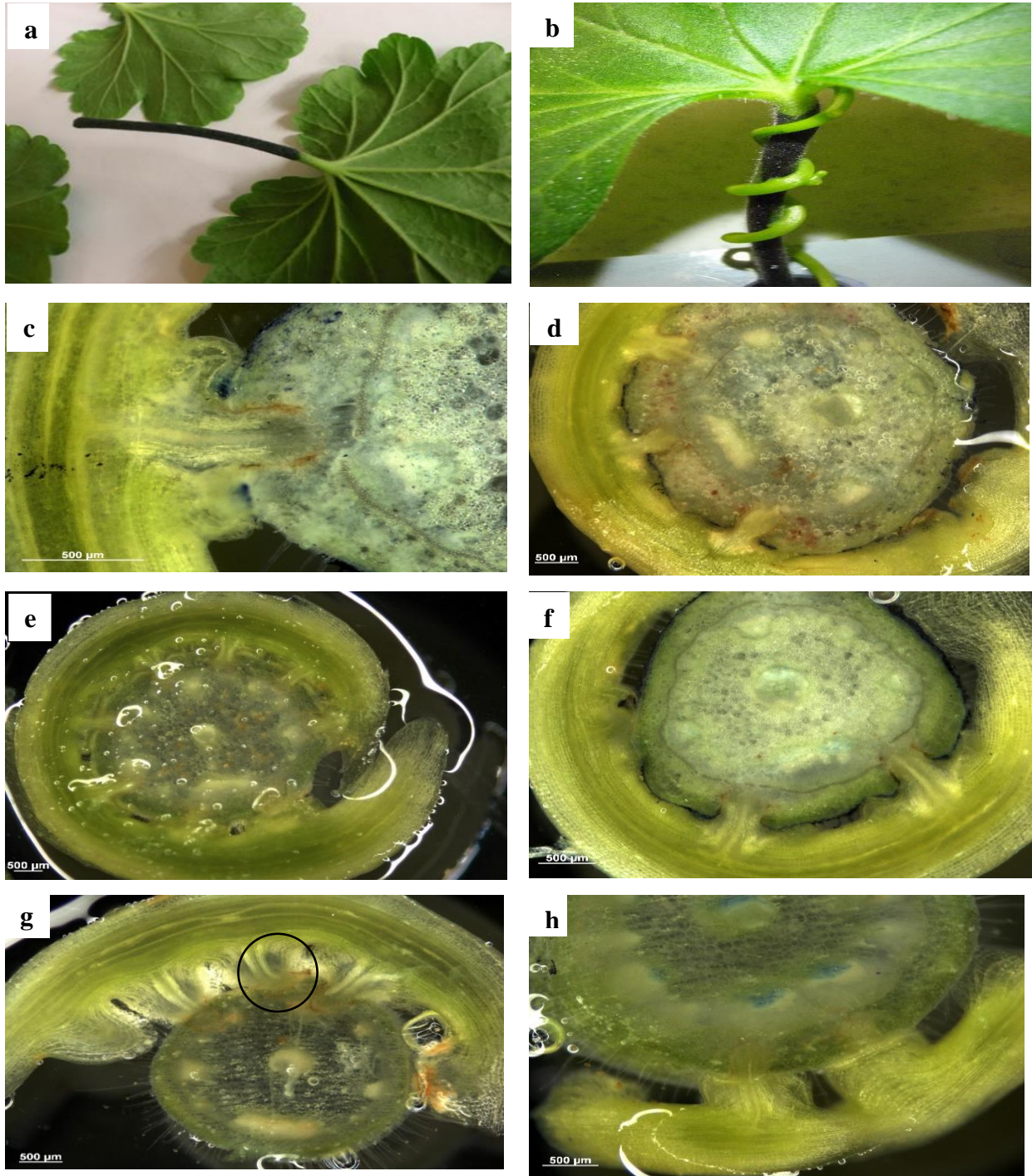


Figure 13- Microscopical cross-sectional views of *C. platyloba* on the *P. zonale*, host petioles coated with BB-R250. Picture “*a-b*” showed petioles coated with BB-R250 and the parasite *C. reflexa* twining around a BB-R250-coated petiole. “*c-f*” depicted cross-sections of *C. platyloba* infecting BB-R250-coated *P. zonale*. “*g-h*” depicted the cross-sections of impeded haustoria in *P. zonale*. Scale bars 500 µm. The circled region in picture “*g*” is as impeded haustorium.

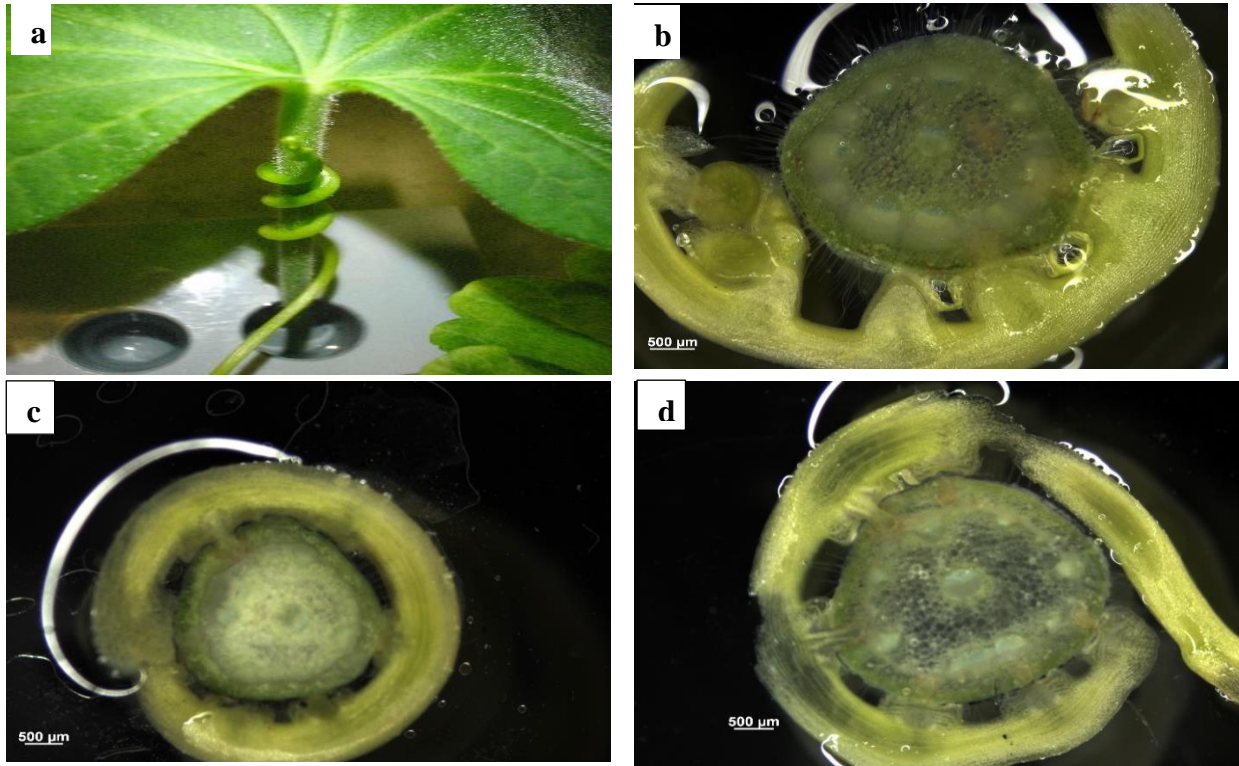


Figure 14- Microscopical cross-sectional views of *C. platyloba* on the *P. zonale*, host petioles coated with 0.005% Poly-L-Lysine. Picture “a” depicted parasite twinning around a 0.005% Poly-L-Lysine-coated petiole (control). “b” young haustoria trying to infuse into host petioles coated with 0.005% Poly-L-Lysine. “c-d” showed cross-sections of infused haustoria into the host petioles.

Table 17- Frequency of impeded *C. platyloba* infections on coated *P. zonale* petioles.

Coat concentration of BB-R250	Total number of sectioned haustoria	Number of prevented penetrations
0	36	1
5mM	38	6

3.7 Enzyme Linked Immuno-Sorbent Assay (ELISA) analysis on *Cuscuta platyloba*

The actual levels of the epitopes of all cell wall hemicellulose and their substituted forms were achieved through the use of monoclonal antibodies which play the roles of locating the specific structural features of the polymers in the context of the haustoria and stem tissue. The rapid screening output of the specificities of individual monoclonal antibodies (mAbs) were displayed in different colour coding patterns which recognised the cell wall hemicellulose components. Within this method, the antigen-specific antibodies LM25 record the hemicellulose analyte of interest and finally converts the substrates into fluorogenic products that are detectable on the ELISA plate reader. After the plate reading (Appendix V, Table 8). In contrast with high fluorescence antibody such as LM25 with low dilution range between 1 and 2 were chosen (Appendix V, Table 9) if there were other monoclonal antibodies to test for their specificities. The analysis is qualitative not quantitative (based on fluorescence figures). Below show the monoclonal antibodies and their binding efficiencies to a series of soluble polysaccharides (the fluorescence signals correspond to the amount of the hemicellulose analyte available in each sample tissue).

MAbs	1 (au)	2 (au)	3 (au)	Dilution	
LM25	1.01	1.00	1.04	1.63	Haustoria
LM25	0.60	0.41	0.35	1.63	Stem
Scale	0	0.25	0.5	0.75	1

Figure 15- The molecule detected by MAb was Xyloglucan. A monoclonal antibody was studied in the cell wall polysaccharides of *Cuscuta platyloba* haustoria and stem tissue samples through ELISA. Result from the heat map depicted, MAb signal from LM25 (Xyloglucan) was present and ranked from highest to lowest across all samples. The control for the background has no antibody which was rated 0 au (level of fluorescence). The experiment was set in mean of three biological replicates, where a cut-off of 0.1 au (level of fluorescence intensity) was removed, any values below this level were regarded as having no signal (-).

4.0 Discussion

In this study, the aim was to draw comparison of the cell walls of two *Cuscuta* species, their different tissues among each other and without including the host cell wall in the analysis (*Pelargonium zonale*). Their activities were tested in different roles in terms of gene expression, XET activities, inhibitory actions with Coomassie BB-R250 and the abundance of hemicelluloses. The expression of cell wall genes and/or abundance rates of the hemicellulose components were of interest in relation to the candidate tissue samples under investigation. The discussion is therefore grouped into four blocks.

The first one addresses the basic influences of the methods on the experimental results (4.1), the correlation of the expression of XTHs among the *Cuscuta* species will be the second part (4.2), the third part is linked to the trial infections with BB-R250 (4.3) and finally, the comparative abundance directed to hemicelluloses in the cell wall of the *Cuscuta* species (4.4).

4.1 Extraction influence on results

The fundamentals of sampling and extraction methods chosen, have crucial effect on results and for that reason, it is very important to be critical about the experimental approaches and one should make it a goal to eliminate contamination in the activities. The extraction stage after the tissue homogenisation can limit the authenticity of the respective methods that follow. That being so, the input quantity and quality are carefully considered through the amplification efficiency and correlation coefficients (R^2) based on the standardized serial dilutions during gene analysis.

Imbeaud et al. (2005) and Raeymaekers (1993) affirmed that high-quality RNA provides desirable gene expression results through the use of RNA isolates with intact bands evident on gel electrophoresis pictures. The sensitivity of RNA quantity and quality is pivotal for deriving relevant gene expression data using real-time qRT-PCR. On that account, the RNA purity as evaluated in Fleige and Pfaffl (2006) is assessed by measuring the A260/280 and A260/230 ratios.

Appendix III (Table 3 and 4) show the RNA purity results of the *Cuscuta campestris* and *Cuscuta platyloba* respectively which confirm the fact that the presence of contaminants that absorb light at a wavelength of 280 nm (nanometres) like for example, protein is insignificant in the isolated *Cuscuta* tissue samples. In contrast, the records of traces of contaminants that absorb light at a

wavelength of 230 nm became a challenge since the assessed results based on the ratio A260/230 appeared to contain such compounds e.g. carbohydrates and phenols but not in excess.

Furthermore, for an excellent gene expression result, the limiting factor that lies on the initial purity of the isolated total RNA (Copois et al. 2007) and purity assessment is also usually based on the presence of intact 28S and 18S ribosomal RNA (Russell and Sambrook 2001). From the results (figure 6), there were clear categorisation of the large and small ribosomal subunits on the gels and this verified that the *Cuscuta* tissue isolates were reliable for such analysis and proven to yield quality gene expression results.

The Livak and Schmittgen (2001) approach works in exponential manner where the cDNA sequence which the qPCR target is in amplified form. As the required efficiency ($E=100\%$) should show, the number of target cDNA molecules doubles every cycle (Adamski et al. 2014). As expected, Figure 8 illustrated the threshold cycle which is drawn from the number of target cDNA molecules for each tissue sample happened to be in accordance with the theory stated above and MIQE guidelines (Bustin et al. 2009). The quantification cycle (C_q) is the intersection between an amplification curve and threshold. The level of fluorescence above the threshold should be set approximately at the same level for all samples. From the experiment, regardless of the number of amplification cycles, each sample crossed the threshold and proved a reliable expression value (Figure7).

4.2 The Gene Expression of XTHs and XET activities in the *Cuscuta* tissue samples

A study conducted by Olsen et al. (2015) discovered the genes *Cr-XTH1* and *Cr-XTH2* (cell wall-modifying enzymes) expressed in *C. reflexa*. The basis of this study was to add-up knowledge about first, the regulation of *XTHs* in *C. campestris* and *C. platyloba*. And again, prove or disprove the hypothesis that these two enzymes are part of a general infection strategy used by the genus *Cuscuta*, irrespective of the species and their host spectra. The focus was on two species that are maintained at the Phytotron at Holt, *C. campestris* and *C. platyloba*.

For gene expression analysis, the optimal standard adopted in this experiment was the quantitative polymerase chain reaction (qPCR) method which stands-out as the most effective method (Adamski et al. 2014). Moreover, the gene expression study of *XTH1* and *XTH2* in *C. campestris*

and *C. platyloba* tissue samples showed differential expression levels in both the young haustoria and stem of the *Cuscuta* samples. In the study of the expression of the cell wall-modifying genes, the *XTH* gene family is known to induce growth, tensile strength and flexibility in plant cell wall in order to withstand environmental stresses (Rose et al. 2002).

For the expression of *XTH1* and *XTH2* in young haustoria and stem tissues of *C. campestris*, *XTH2* was highly expressed in both the stem tissues and young haustoria, with a slightly higher expression in stems (figure 9 a). There was about 1.6 fold-higher expression of *XTH2* in the stem than the young haustoria sections of *C. campestris* but *XTH1* was not found to be expressed in *C. campestris*.

In contrast, in *C. platyloba*, *XTH1* was actively expressed in the young haustoria section but no traces of regulation of *XTH1* in the stem region. The gene *XTH1* displayed the highest differential expression levels, with changes of approximately 28 fold-higher expression in the haustoria than stem but very little expression of *XTH2* in the haustoria and stem regions. Interestingly, the expression results does not totally conform to the study by Olsen et al. (2015) in that only the closet homologue to *Cr-XTH2* in *C. campestris* (*Cc-XTH2*) was more highly expressed in the stem than in the haustoria but no expression of *Cc-XTH1* was observed in both sections of the species. Further analysis of the gene expression in *C. platyloba* was contrary to the same report.

According to the study and in reference to the three main parasitic infection stages of *Cuscuta* species, the genes *XTH1* and *XTH2* are highly detectable at the initial stage of the haustorium development (Olsen et al. 2015) which is termed as “the young haustorium” in this experiment. The presence of XET, cell wall-modifying enzymes cause the loosening of plant cell wall by splitting and grafting to other microfibrils chains and this loosening process do not make it permanently closed border for invasion (Olsen and Krause 2017).

The differential expression levels of XTHs in the haustoria and stem regions of both *C. campestris* and *C. platyloba* can be explained in their phylogenetic perspective in relation to *C. reflexa*. A consensus tree generated from the plastid *rbcL* showed more distant relationship between *C. campestris* and *C. reflexa* than between *C. platyloba* and *C. reflexa* (personal communication, data not shown). In this account, the observed expression of XTHs to be upregulated in the young haustoria of *C. reflexa* (Olsen et al. 2015) could further argue for the fact that XTH upregulated in stem tissue than haustoria in *C. campestris* does not totally play the role of cell wall loosening

process (Olsen and Krause 2017). Other arguments could be that XTHs in *C. campestris* are rather very active in stem elongation but not in haustoria growth which is contrary to the report from Olsen and Krause (2017). This is not the case in *C. platyloba* which is more closely related to *C. reflexa*. Some extra difference can be also drawn from the subgenus of the two species, where *C. reflexa* is found in the subgenus *Monogyna* (photosynthetically active group) and *C. campestris* in the subgenus *Grammica* (basically a low to no chlorophyll group).

XET activity correlated to the roles of cell expansion or wall restructuring and measurements in *C. platyloba* and *C. campestris* (section 3.5.2), showed high levels of XET action in both species.

Graphical representation and mean separation further confirmed the significant fluorescence within and between the *Cuscuta* species. Thus, no significant fluorescence difference was observed within the *C. platyloba* and *C. campestris* haustoria and stem regions, but vice versa between them. Hence, the activity is predominant when cell walls are restructuring e.g. in the young haustorium region. There was a reversed observation of XET activity when normalized per protein concentration which showed no significant differences within and between the species. This is evident in the study of XET activity in *C. reflexa* (Olsen and Krause 2017) where there were higher activities in penetrating haustoria than in other tested regions of the parasite. As recorded in Olsen et al. (2015) the elongating cells are predominant in regions of high xyloglucan-modifying enzymes and this morphological changes correlate to the roles of XTHs. In this, the increased XET activity and the appearance of high fluorescence are active during the initial growth stages of the haustoria (Olsen and Krause 2017). The pattern of XET action indicates the modification of xyloglucans which function in plant development. Again, during the haustorium-host invasion, xyloglucan modifications is needed to assist the process through host cell wall loosening activities and this working hypothesis is evident in the gene expression analysis in *C. platyloba*. In relation to other analysis, there is unparallel correlations between protein concentration and XET activity levels in the *Cuscuta* stem tissue. This happens if the values (the mean adj. vol.) are normalised per protein concentration. The XET activity appears to be higher in the stem than haustoria per mg protein but the differences are not significant.

4.3 Infection Trials with Coomassie Brilliant Blue R 250 (BB-R250)

Chormova et al. (2015) identified Coomassie Brilliant Blue R 250 as an inhibitor for activity of XET in parsley through the study of screens for xenobiotics. By coating this compound on to the petioles of the susceptible host, *P. zonale*, followed by several infection trials with *Cuscuta* species, the presence of BB-R250 succeeded partially to lower successful haustoria penetration into the host tissue in *C. reflexa* (Olsen and Krause 2017). Some obvious reason of failure to completely inhibit infection could be the poor adhesion of BB-R250 (although the solution was supplemented with Poly-L-Lysine) as previously stated in “*section 2.5, Figure 5*” and host-surface hydrophobicity (Olsen and Krause 2017). The above observation was similar to the experiment conducted on *C. platyloba*. In *C. platyloba*, successful haustoria infection into the host was approximately 88% under a concentration of 5mM of BB-R250 and 97% infection-rate in where Poly-L-Lysine (control) were applied, which showed that the inhibition of haustoria growth in *C. platyloba* into the host tissue could neither be dependant on the hydrophilic nature of the type of inhibitor nor the hydrophobic surface of the petioles (Olsen and Krause 2017). Overall, coating the host petioles with small inhibitor such as Coomassie Brilliant Blue R 250 did not completely suppress the ability of haustoria of *C. platyloba* infection rate, but this needs to be investigated further.

4.4 Abundance of Xyloglucan in the *Cuscuta* cell wall

The compositional differences of cell walls of stem and haustorium were reported in some studies (Johnsen et al. 2015). In the present study, only the xyloglucan epitope (recognised by mAb LM25) was investigated. It was shown to be more abundant in haustoria than in stem regions. The high presence of xyloglucan in the haustorial extract links its association to the high expression of XTHs. This could imply that the parasite, *C. platyloba*, could indeed contribute to some structural alteration in the cell wall. And such cell restructuring process can cause an elongation action that can lead to the formation of the specialised structure called haustoria. Generally, high abundance of mAb LM25 is in unison with the findings by Scheller and Ulvskov (2010) that classified xyloglucan to be most abundant hemicellulose and that xyloglucans are mostly abundant in areas of plants where many cell expansion processes occur e.g. root tips (Rose et al. 2002). But the parallel correlation between XTHs and xyloglucan in the haustorial region is not the same as in the stem of the parasite in terms of XET activity. The XET activity being lower in the haustorium than

in the stem does not mean that the activity can not be essential to haustorium development. It just shows that there is also activity in both tissues, and at a higher level in the stem. The low XET activity in the haustoria compared to the stem could be a reason of masking. During the process of masking, the epitope xyloglucan is shielded from monoclonal antibodies detection by pectic homogalacturonan (HG) and the polymer will only be detectable after HG removal by pectinases (Marcus et al. 2008; Hervé et al. 2009). It can therefore be verified from this study that the haustorial organ of *C. platyloba* makes full use of xyloglucan, while in the stem region it does not seem to play the same role. This can also support the role it plays regarding the parasitization of the host cell wall.

5.0 Conclusion

Cuscuta is a complex parasitic plant that has gained global relevance by threatening the existence of plants, thus the need for their investigation and control. In conclusion, this investigation has revealed that;

The different groups of XTHs may have varied functions and multiple sites of action in the different species of *Cuscuta*, thus affecting the different levels of XTH expression in the haustoria and stems of both *C. campestris* and *C. platyloba*. XET activity on the other hand, is high per mg of tissue sample in the haustoria of *C. campestris* but higher in stem per proteins concentration. In whatever way, the activity of XET remained high when normalized per mg tissue sample or per protein concentration in *C. platyloba* and this may imply that additional XTHs (thus, not only *XTH1* and *XTH2* as tested) could be expressed as well to account for the high XET activity in both the *Cuscuta* species.

The cell wall component of *C. platyloba* contained high levels of xyloglucan tentatively indicating the significance of remodeling activity in the parasite. Trials to inhibit infection with XET inhibitors need to be extended before comparative conclusions can be drawn.

5.1 Outlook

Similar research works need to be extended to the other species such as *Cuscuta campestris* in order to investigate the inhibitory actions of BB-R250 in the development of the haustoria structure. Also, the inhibitory effect of BB-R250 on XET activity should be checked on extracts of *C. campestris* and *C. platyloba* in vitro.

Studies about the hemicellulose compositional differences in the cell wall should be further embarked upon. As revealed from literature, some hemicelluloses such as xyloglucan and xylan can be poorly represented in the cell walls because of masking by pectic homogalacturonan. To eradicate such problems, the pectic homogalacturonan should be removed from the cell wall tissues with a Pectate lyase (Pel 10A) before immunolabelling.

6.0 References

- Adamski MG, Gumann P, Baird AE (2014)** A method for quantitative analysis of standard and high-throughput qPCR expression data based on input sample quantity. *PloS one* 9 (8):e103917.
- Albert M, Belastegui-Macadam XM, Bleischwitz M, Kaldenhoff R (2008)** *Cuscuta* spp:“Parasitic plants in the spotlight of Plant Physiology, Economy and Ecology”. In: *Progress in Botany*. Springer, pp 267-277.
- Albert M, Werner M, Proksch P, Fry S, Kaldenhoff RJPB (2004)** The cell wall-modifying xyloglucan endotransglycosylase/hydrolase LeXTH1 is expressed during the defence reaction of tomato against the plant parasite *Cuscuta reflexa*. *6 (04):402-407*.
- Barkman TJ, McNeal JR, Lim S-H, Coat G, Croom HB, Young NDJBEB (2007)** Mitochondrial DNA suggests at least 11 origins of parasitism in angiosperms and reveals genomic chimerism in parasitic plants. *7 (1):248*.
- Begon M, Townsend CR, Harper JL (2006)** *Ecology: from individuals to ecosystems*. vol Sirsi) i9781405111171.
- Bidartondo MIJNP (2005)** The evolutionary ecology of myco-heterotrophy. *167 (2):335-352*.
- Birschwilks M, Haupt S, Hofius D, Neumann SJJoEB (2006)** Transfer of phloem-mobile substances from the host plants to the holoparasite *Cuscuta* sp. *57 (4):911-921*.
- Bringmann C, Schlauer J, Rückert M, Wiesen B, Ehrenfeld K, Proksch P, Czygan FCJPB (1999)** Host-Derived Acetogenins Involved in the Incompatible Parasitic Relationship between *Cuscuta reflexa* (Convolvulaceae) and *Ancistrocladus heyneanus* (Ancistrocladaceae) 1. *1 (5):581-584*.
- Bustin SA, Benes V, Garson JA, Hellemans J, Huggett J, Kubista M, Mueller R, Nolan T, Pfaffl MW, Shipley GL (2009)** The MIQE guidelines: minimum information for publication of quantitative real-time PCR experiments. *Clinical chemistry* 55 (4):611-622
- Campbell P, Braam J (1999)** Xyloglucan endotransglycosylases: diversity of genes, enzymes and potential wall-modifying functions. *Trends in plant science* 4 (9):361-366
- Capderon M, Fer A, Ozenda PJCRdlAdSSSdlV (1985)** About an unreported system leading to the expulsion of a parasite: *Cuscuta* on cotton-plant (*Cuscuta lupuliformis* Krock. on *Gossypium hirsutum* L.)[resistance to pathogen dicotyledons].

- Chebli Y, Geitmann A (2017)** Cellular growth in plants requires regulation of cell wall biochemistry. *Current opinion in cell biology* 44:28-35.
- Chormova D, Franková L, Defries A, Cutler SR, Fry SC (2015)** Discovery of small molecule inhibitors of xyloglucan endotransglucosylase (XET) activity by high-throughput screening. *Phytochemistry* 117:220-236.
- Christensen NM, Dörr I, Hansen M, Van Der Kooij T, Schulz AJP (2003)** Development of *Cuscuta* species on a partially incompatible host: induction of xylem transfer cells. 220 (3-4):131-142.
- Copois V, Bibeau F, Bascoul-Mollevi C, Salvetat N, Chalbos P, Bareil C, Candeil L, Fraslon C, Conseiller E, Granci V (2007)** Impact of RNA degradation on gene expression profiles: assessment of different methods to reliably determine RNA quality. *Journal of biotechnology* 127 (4):549-559.
- Cosgrove DJ (2005)** Growth of the plant cell wall. *Nature reviews molecular cell biology* 6 (11):850.
- Dawson JH, Musselman LJ, Wolswinkel P, Dörr IJRoWS (1994)** Biology and control of *Cuscuta*. 6:265-317.
- Ellison AM, Gotelli NJJJoEB (2009)** Energetics and the evolution of carnivorous plants—Darwin's 'most wonderful plants in the world'. 60 (1):19-42.
- Fleige S, Pfaffl MW (2006)** RNA integrity and the effect on the real-time qRT-PCR performance. *Molecular aspects of medicine* 27 (2-3):126-139.
- Fry SCJTPJ (1997)** Novel 'dot-blot' assays for glycosyltransferases and glycosylhydrolases: optimization for xyloglucan endotransglycosylase (XET) activity. 11 (5):1141-1150.
- Furuhashi T, Furuhashi K, Weckwerth WJJopi (2011)** The parasitic mechanism of the holostemparasitic plant *Cuscuta*. 6 (4):207-219.
- García MA, Costea M, Kuzmina M, Stefanović SJAjob (2014)** Phylogeny, character evolution, and biogeography of *Cuscuta* (dodders; Convolvulaceae) inferred from coding plastid and nuclear sequences. 101 (4):670-690.
- Hegenauer V, Fürst U, Kaiser B, Smoker M, Zipfel C, Felix G, Stahl M, Albert MJS (2016)** Detection of the plant parasite *Cuscuta reflexa* by a tomato cell surface receptor. 353 (6298):478-481.
- Heide-Jørgensen H (2008)** Parasitic flowering plants. Leiden, The Netherlands: Brill.

- Hervé C, Rogowski A, Gilbert HJ, Paul Knox J (2009)** Enzymatic treatments reveal differential capacities for xylan recognition and degradation in primary and secondary plant cell walls. *The Plant Journal* 58 (3):413-422.
- Hibberd JM, Dieter Jeschke WJ, Joeb (2001)** Solute flux into parasitic plants. *Plant, Cell & Environment* 24 (363):2043-2049.
- Imbeaud S, Graudens E, Boulanger V, Barlet X, Zaborski P, Eveno E, Mueller O, Schroeder A, Auffray C (2005)** Towards standardization of RNA quality assessment using user-independent classifiers of microcapillary electrophoresis traces. *Nucleic acids research* 33 (6):e56-e56.
- Jiang L, Wijeratne AJ, Wijeratne S, Fraga M, Meulia T, Doohan D, Li Z, Qu F, JPO (2013)** Profiling mRNAs of two *Cuscuta* species reveals possible candidate transcripts shared by parasitic plants. *PLoS ONE* 8 (11):e81389.
- Johnsen HR, Striberny B, Olsen S, Vidal-Melgosa S, Fangel JU, Willats WG, Rose JK, Krause K, JNP (2015)** Cell wall composition profiling of parasitic giant dodder (*Cuscuta reflexa*) and its hosts: a priori differences and induced changes. *Plant, Cell & Environment* 38 (3):805-816.
- Kaiser B, Vogg G, Fürst UB, Albert MJ, Fips (2015)** Parasitic plants of the genus *Cuscuta* and their interaction with susceptible and resistant host plants. *Plant, Cell & Environment* 38 (1):6-16.
- Leake JR, JNP (1994)** The biology of myco-heterotrophic ('saprophytic') plants. *Plant, Cell & Environment* 17 (2):171-216.
- Livak KJ, Schmittgen TD (2001)** Analysis of relative gene expression data using real-time quantitative PCR and the $2^{-\Delta\Delta CT}$ method. *Methods* 25 (4):402-408.
- Marcus SE, Verherbruggen Y, Hervé C, Ordaz-Ortiz JJ, Farkas V, Pedersen HL, Willats WG, Knox JP (2008)** Pectic homogalacturonan masks abundant sets of xyloglucan epitopes in plant cell walls. *BMC plant biology* 8 (1):60.
- Mayer AJP (2006)** Pathogenesis by fungi and by parasitic plants: similarities and differences. *Plant, Cell & Environment* 29 (1):3-16.
- McNeal JR, Arumugunathan K, Kuehl JV, Boore JL, JBb (2007)** Systematics and plastid genome evolution of the cryptically photosynthetic parasitic plant genus *Cuscuta* (Convolvulaceae). *Plant, Cell & Environment* 30 (1):55.
- Merckx V, Bidartondo MI, Hynson NA, JAoB (2009)** Myco-heterotrophy: when fungi host plants. *Plant, Cell & Environment* 32 (7):1255-1261.

- Mishra J, Moorthy B, Gogoi A (2006)** Biology and Management of Cuscuta. Director, National Research Centre for Weed Science.
- Mota TR, de Oliveira DM, Marchiosi R, Ferrarese-Filho O, dos Santos WD (2018)** Plant cell wall composition and enzymatic deconstruction. *AIMS BIOENGINEERING* 5 (1):63-77.
- Muñoz-Bertomeu J, Lorences EP (2014)** Changes in xyloglucan endotransglucosylase/hydrolase (XTHs) expression and XET activity during apple fruit infection by *Penicillium expansum* Link. *A. European journal of plant pathology* 138 (2):273-282.
- Nishitani K, Tominaga R (1992)** Endo-xyloglucan transferase, a novel class of glycosyltransferase that catalyzes transfer of a segment of xyloglucan molecule to another xyloglucan molecule. *Journal of Biological Chemistry* 267 (29):21058-21064.
- Okazawa K, Sato Y, Nakagawa T, Asada K, Kato I, Tomita E, Nishitani K (1993)** Molecular cloning and cDNA sequencing of endoxyloglucan transferase, a novel class of glycosyltransferase that mediates molecular grafting between matrix polysaccharides in plant cell walls. *Journal of Biological Chemistry* 268 (34):25364-25368.
- Olsen S, Krause KJPo (2017)** Activity of xyloglucan endotransglucosylases/hydrolases suggests a role during host invasion by the parasitic plant *Cuscuta reflexa*. 12 (4):e0176754.
- Olsen S, Striberny B, Hollmann J, Schwacke R, Popper Z, Krause K (2015)** Getting ready for host invasion: elevated expression and action of xyloglucan endotransglucosylases/hydrolases in developing haustoria of the holoparasitic angiosperm *Cuscuta*. *Journal of experimental botany* 67 (3):695-708.
- Pedersen HL, Fangel JU, McCleary B, Ruzanski C, Rydahl MG, Ralet M-C, Farkas V, von Schantz L, Marcos SE, Andersen MCJJoBC (2012)** Versatile high-resolution oligosaccharide microarrays for plant glycobiology and cell wall research.jbc. M112. 396598.
- Poulin R (2011)** The many roads to parasitism: a tale of convergence. In: *Advances in parasitology*, vol 74. Elsevier, pp 1-40.
- Press MC, Phoenix GKJNp (2005)** Impacts of parasitic plants on natural communities. 166 (3):737-751.
- Raeymaekers L (1993)** Quantitative PCR: theoretical considerations with practical implications. *Analytical biochemistry* 214 (2):582-585.

- Ranjan A, Ichihashi Y, Farhi M, Zumstein K, Townsley B, David-Schwartz R, Sinha NRJPP (2014)** De novo assembly and characterization of the transcriptome of the parasitic weed dodder identifies genes associated with plant parasitism. 166 (3):1186-1199.
- Rose JK, Braam J, Fry SC, Nishitani KJP, Physiology C (2002)** The XTH family of enzymes involved in xyloglucan endotransglucosylation and endohydrolysis: current perspectives and a new unifying nomenclature. 43 (12):1421-1435.
- Runyon JB, Mescher MC, De Moraes CM (2006)** Volatile chemical cues guide host location and host selection by parasitic plants. Science 313 (5795):1964-1967.
- Runyon JB, Mescher MC, De Moraes CMJPP (2008)** Parasitism by *Cuscuta pentagona* attenuates host plant defenses against insect herbivores. 146 (3):987-995.
- Runyon JB, Mescher MC, Felton GW, De Moraes CMJP, cell, environment (2010)** Parasitism by *Cuscuta pentagona* sequentially induces JA and SA defence pathways in tomato. 33 (2):290-303.
- Russell DW, Sambrook J (2001)** Molecular cloning: a laboratory manual, vol 1. Cold Spring Harbor Laboratory Cold Spring Harbor, NY.
- Scheller HV, Ulvskov P (2010)** Hemicelluloses. Annual review of plant biology 61.
- Sharples SC, Nguyen-Phan TC, Fry SC (2017)** Xyloglucan endotransglucosylase/hydrolases (XTHs) are inactivated by binding to glass and cellulosic surfaces, and released in active form by a heat-stable polymer from cauliflower florets. Journal of plant physiology 218:135-143.
- Stefanović S, Kuzmina M, Costea MJAJoB (2007)** Delimitation of major lineages within *Cuscuta* subgenus *Grammica* (Convolvulaceae) using plastid and nuclear DNA sequences. 94 (4):568-589.
- Van Sandt VS, Suslov D, Verbelen J-P, Vissenberg K (2007)** Xyloglucan endotransglucosylase activity loosens a plant cell wall. Annals of Botany 100 (7):1467-1473.
- Werner M, Uehlein N, Proksch P, Kaldenhoff RJP (2001)** Characterization of two tomato aquaporins and expression during the incompatible interaction of tomato with the plant parasite *Cuscuta reflexa*. 213 (4):550-555.
- Westwood JH, Yoder JI, Timko MPJTips (2010)** The evolution of parasitism in plants. 15 (4):227-235.

- Wikström N, Savolainen V, Chase MWJPotRSoLSBBS (2001)** Evolution of the angiosperms: calibrating the family tree. 268 (1482):2211-2220.
- Xu W, Campbell P, Vargheese AK, Braam J (1996)** The Arabidopsis XET-related gene family: environmental and hormonal regulation of expression. The Plant Journal 9 (6):879-889.
- Yokoyama R, Nishitani K (2001)** A comprehensive expression analysis of all members of a gene family encoding cell-wall enzymes allowed us to predict cis-regulatory regions involved in cell-wall construction in specific organs of Arabidopsis. Plant and Cell Physiology 42 (10):1025-1033.
- Yoshida S, Cui S, Ichihashi Y, Shirasu KJARoPB (2016)** The haustorium, a specialized invasive organ in parasitic plants. 67:643-667.
- Yoshida S, Shirasu KJCoipb (2012)** Plants that attack plants: molecular elucidation of plant parasitism. 15 (6):708-713.
- Yuncker TGJMotTBC (1932)** The genus Cuscuta. 18 (2):109-331.

7.0 Appendix I

Table 1- Gene-specific primers for *Cuscuta campestris* and *Cuscuta platyloba* with respective amplicon sizes which ranged from 75-250 bp and dilution volume for each sample.

Gene Symbol	Amplicon Size (bp)	μL for 100 μM
<i>Cuscuta campestris</i>		
<i>Cc-XTH1</i>	137	F- 779 R-1129
<i>Cc-XTH2</i>	133	F- 797 R-1203
<i>Cuscuta platyloba</i>		
<i>Cp-XTH1</i>	79	F- 789 R- 884
<i>Cp-XTH2</i>	219	F- 645 R- 646
<i>Cp-Actin</i>	228	F- 642 R- 644
<i>Cp-EF1α</i>	156	F- 651 R- 758
<i>Cp-G6PD</i>	145	F- 709 R- 687
<i>Cp-SF2</i>	128	F- 738 R- 555

7.1 Appendix II

Table 2- Overall Reaction volumes for DNase Treatment for *Cuscuta* species samples.

**Cuscuta campestris* **Cuscuta platyloba* **Haustoria* tissue sample *Stem tissue sample.

*CcH- *Cuscuta campestris haustoria* *CcS- *Cuscuta campestris* stem *CpH-*Cuscuta platyloba haustoria*

*CpS-*Cuscuta platyloba* Stem.

Type of <i>Cuscuta</i> Tissue sample	Vol. of 10× DNase I Buffer (μL)	Vol. of rDNase 1 (μL)	Vol. of Total RNA (μL)	Vol. of RNase-free Water (μL)
CcH1	2	1	11.6	5.4
CcH2	2	1	13.8	3.2
CcH3*	2	1	17.1	-
CcS1	2	1	14.1	2.9
CcS2*	3.4	1	30.0	-
CcS3*	2	1	18.6	-
CpH1*	2.5	1	21.4	-
CpH2	2	1	10.9	6.1
CpH3	2	1	15.4	1.6
CpS1*	2	1	17.8	-
CpS2*	3	1	24.0	2
CpS3	2	1	13.3	3.7

7.2 Appendix III

Table 3- Quality Assessment and Concentration Results of Total RNA in *Cuscuta Campestris*. The values from Table 3 and 4 shows insignificant the levels of contaminants which absorb light wavelength at 280 nm but very little traces of contaminants which absorb light at 230 nm.

Sample Name	Concentration (ng/μl)	260/280	260/230
Haustoria 1	172.1	2.11	2.12
Haustoria 2	146.2	2.11	2.13
Haustoria 3	116.9	2.11	1.91
Stem 1	141.5	2.09	1.80
Stem 2	47.8	2.06	1.91
Stem 3	107.4	2.15	1.43

Table 4- Quality Assessment and Concentration Results of Total RNA in *Cuscuta platyloba*.

Sample Name	Concentration (ng/μl)	260/280	260/230
Haustoria 1	183.1	2.14	1.23
Haustoria 2	129.7	2.10	1.62
Haustoria 3	201.6	2.10	1.93
Stem 1	112.2	2.09	1.67
Stem 2	101.4	2.06	1.79
Stem 3	150.9	2.12	1.83

7.3 Appendix IV

Table 5- Records of BSA Dilution Series (mg/ml) and absorbance (A).

Dilution Series (mg/ml)	Absorbance (A)
1	0.955
0.8	0.768
0.6	0.590
0.4	0.460
0.2	0.259

Table 6- Raw data extrapolated for Graphical Representation of XTH activity in *C. platyloba* (Cp) and *C. campestris* (Cc) (when Normalised per mg of tissue samples) respectively.

A.

Sample level	Replicate I	Replicate II	Replicate III	Adj. Vol. (Int)	Tol. Avg. Adj. Vol. (Int)
<i>Cp</i> H1	50169120	94593792	60492024	68418312	88124355.11
<i>Cp</i> H2	90878260	121928636	100726224	104511040	
<i>Cp</i> H3	72105696	104278396	97947048	91443713.33	
<i>Cp</i> S1	80999944	124449288	80190788	95213340	94463616
<i>Cp</i> S2	107302852	121297336	95581152	108060446.7	
<i>Cp</i> S3	77368104	89570520	73412560	80117061.33	

B.

Sample level	Replicate I	Replicate II	Replicate III	Adj. Vol. (Int)	Tol. Avg. Adj. Vol. (Int)
Cc H1	160094544	194921776	102554816	152523712	198444426.7
Cc H2	288636556	308843712	234640912	277373726.7	
Cc H3	158643804	186904064	150759656	165435841.3	
Cc S1	203163728	231873960	132171684	189069790.7	172721325.8
Cc S2	281725864	263717688	206283732	250575761.3	
Cc S3	82425496	79825548	73304232	78518425.33	

Table 7- Raw data extrapolated for Graphical Representation of XTH activity in *C. platyloba* (Cp) and *C. campestris* (Cc) (when Normalised per protein concentration) respectively.

Sample level	Total Avg. Adj vol. (Int.)	Total Avg. Protein Concentration	Activity per Protein Concentration)
Cp H	88124355.11	1.5420333	57952347.01
Cp S	94463616	0.7515333	132950468.8
Cc H	198444426.7	1.5199333	130163393
Cc S	172721325.8	0.73	237534225.2

7.4 Appendix V

Table 8- Accumulated data for *C. platyloba* haustoria data analysis.

H1

	LM12			LM21			LM25		
A	0.055	0.057	0.054	0.073	0.074	0.075	2.245	2.358	2.396
B	0.054	0.059	0.053	0.097	0.102	0.103	2.225	2.297	2.167
C	0.064	0.064	0.061	0.088	0.085	0.091	2.16	2.098	2.364
D	0.058	0.059	0.058	0.056	0.063	0.063	1.603	1.593	1.567
E	0.055	0.055	0.066	0.052	0.06	0.063	1.066	0.902	1.063
F	0.059	0.054	0.067	0.05	0.054	0.058	0.486	0.335	0.511
G	0.06	0.06	0.066	0.051	0.056	0.077	0.212	0.194	0.267
H	0.065	0.064	0.062	0.058	0.051	0.058	0.075	0.073	0.075

H2

	LM12			LM21			LM25		
A	0.055	0.054	0.063	0.064	0.064	0.066	1.737	1.863	1.788
B	0.05	0.05	0.051	0.102	0.104	0.108	1.854	2.139	2.056
C	0.056	0.052	0.054	0.073	0.078	0.076	1.979	1.784	1.859
D	0.056	0.051	0.065	0.054	0.056	0.057	1.767	1.506	1.53
E	0.055	0.054	0.056	0.051	0.052	0.051	0.943	1.001	1.034
F	0.055	0.053	0.054	0.051	0.051	0.049	1.11	0.182	0.21
G	0.054	0.053	0.054	0.053	0.047	0.052	0.144	0.147	0.146
H	0.054	0.053	0.055	0.039	0.053	0.049	0.062	0.061	0.065

H3

	LM12			LM21			LM25		
A	0.051	0.051	0.052	0.063	0.059	0.064	1.964	1.959	1.975
B	0.053	0.049	0.05	0.073	0.075	0.071	2.05	1.919	1.908
C	0.053	0.05	0.052	0.066	0.065	0.086	1.792	1.672	1.849
D	0.059	0.061	0.058	0.056	0.058	0.056	1.523	1.545	1.564
E	0.059	0.055	0.054	0.054	0.054	0.053	1.02	1.052	1.033
F	0.055	0.053	0.055	0.052	0.05	0.206	0.478	0.434	0.453
G	0.054	0.058	0.069	0.05	0.051	0.118	0.194	0.154	0.195
H	0.062	0.055	0.056	0.052	0.049	0.051	0.063	0.053	0.058

Table 9- Accumulated data for *C. platyloba* stem data analysis.

S1

	LM11			LM22			LM25		
A	0.472	0.541	0.422	0.052	0.047	0.056	1.826	1.667	1.766
B	0.52	0.477	0.468	0.048	0.047	0.05	1.909	1.765	1.822
C	0.294	0.338	0.273	0.047	0.049	0.048	1.735	1.331	1.59
D	0.111	0.1	0.1	0.048	0.045	0.048	1.216	1.095	1.376
E	0.06	0.066	0.056	0.049	0.044	0.047	0.681	0.49	0.576
F	0.053	0.059	0.053	0.048	0.046	0.047	0.217	0.213	0.252
G	0.055	0.048	0.05	0.049	0.048	0.05	0.174	0.18	0.213
H	0.05	0.045	0.05	0.047	0.052	0.048	0.077	0.074	0.092

S2

	LM11			LM22			LM25		
A	0.147	0.165	0.091	0.051	0.045	0.046	1.697	1.701	1.636
B	0.215	0.175	0.148	0.046	0.047	0.045	1.803	1.808	1.81
C	0.15	0.126	0.136	0.047	0.044	0.046	1.324	1.411	1.472
D	0.086	0.067	0.07	0.047	0.045	0.047	0.912	0.926	0.99
E	0.051	0.051	0.052	0.047	0.045	0.045	0.382	0.437	0.423
F	0.051	0.048	0.047	0.048	0.047	0.048	0.165	0.184	0.161
G	0.053	0.052	0.048	0.051	0.047	0.047	0.113	0.116	0.112
H	0.063	0.051	0.047	0.047	0.049	0.054	0.065	0.064	0.063

S3

	LM11			LM22			LM25		
A	0.216	0.198	0.163	0.052	0.05	0.052	1.544	1.508	1.5
B	0.181	0.158	0.164	0.047	0.046	0.045	1.623	1.493	0.12
C	0.244	0.228	0.217	0.046	0.045	0.046	1.513	1.329	0.09
D	0.129	0.106	0.091	0.048	0.043	0.051	1.3	0.857	0.079
E	0.062	0.068	0.059	0.047	0.045	0.047	0.619	0.343	0.073
F	0.052	0.057	0.055	0.046	0.055	0.048	0.263	0.178	0.074
G	0.054	0.055	0.057	0.047	0.045	0.047	0.218	0.13	0.067
H	0.07	0.058	0.066	0.049	0.066	0.049	0.073	0.068	0.069